2018

Mapping and Risk Assessment of Juniper Encroachment Into a Prairie Landscape

Kyle D. Kaskie
South Dakota State University

MAPPING AND RISK ASSESSMENT OF JUNIPER ENCROACHMENT INTO A PRAIRIE LANDSCAPE

BY

KYLE D. KASKIE

A thesis submitted in partial fulfillment of the requirements for the

Master of Science

Specialization in Biology

Major in Biological Sciences

South Dakota State University

2018

MAPPING AND RISK ASSESSMENT OF JUNIPER ENCROACHMENT INTO A PRAIRIE LANDSCAPE

This thesis is approved as a creditable and independent investigation by a candidate for the Master of Science in Biological Science degree and is acceptable for meeting the thesis requirements for this degree. Acceptance of this thesis does not imply that the conclusions reached by the candidate are necessarily the conclusions of the major department.

Michael C. Wimberly, Ph.D. Date
Thesis Advisor

Michele R. Dudash, Ph.D. Date
Head, Department of Natural Resource Management

Kimchel C. Doerner, Ph.D. Date
Dean, Graduate School

ACKNOWLEDGEMENTS

I want to begin by thanking my parents, Kenneth and Sandra Kaskie. I would not be where I am today without all of the love and guidance you have given me over the years. You have allowed me to pursue my passions in the outdoors and continue to support my every step. I would also like to thank my sister, Breanna, for everything you have done for me over these years.

I thank my love, Bailey, for all of your love and support along this journey. You have always been there for me, sharing in the same dreams and goals in life. You have put up with all of my nonsense and still love me for it. I cannot wait to spend many more years with you by my side.

I would like to thank my advisor, Dr. Michael C. Wimberly, for giving me this opportuning and allowing me to pursue the next step in my education. I appreciate all of your help and support throughout my graduate school experience. You have been a huge help in the development of my thesis. I will apply everything I have learned along the way in my next career path.

I would like to thank Pete Bauman, for giving me the opportunity in developing this project. You have worked with me to make this all happen and I owe you a debt gratitude for it. I also thank the rest of my committee, Dr. Joshua Leffler and graduate faculty representative Dr. Rocky Dailey.

Lastly, I would like to thank my lab members Andrea Hess, Dawn Nekorchuk, and Francis Dwomoh, for your comments and suggestions along the way. I give special thanks to my office mate, Justin Davis, for all of your knowledge and statistical guidance.

Funding and support for this project was provided by Geospatial Sciences Center of Excellence, South Dakota State University.

CONTENTS

LIST OF FIGURES

LIST OF TABLES

LIST OF APPENDICES

ABSTRACT

MAPPING AND RISK ASSESSMENT OF JUNIPER ENCROACHMENT INTO A PRAIRIE LANDSCAPE

KYLE D. KASKIE

2018

Juniper encroachment is a considerable threat to the prairie ecosystems of the Great Plains because it has the potential to alter native grasslands by changing soil characteristics, limiting herbaceous biomass, and hindering native community regeneration. Accurate maps of juniper cover and predictions of areas at risk for future expansion are needed to support proactive management measures. Therefore, our objectives are to: (1) Develop a practical workflow for large-scale juniper mapping using Landsat 8 Operational Land Imager (OLI) imagery and partial unmixing techniques, (2) Compare the classification accuracies from the resulting map based on different juniper density thresholds and different types of imagery, (3) Develop a predictive spatial model for the distribution of low-density juniper based on distance to seed source and environmental covariates and determine the prediction accuracy, and (4) Use the resulting maps to evaluate the extent of current juniper establishment and the risk of future encroachment. The study area encompasses counties bordering the Missouri River in southeastern South Dakota and northeastern Nebraska and covering approximately 23,000 km^2. We applied a matched filtering technique to classify juniper with snow-covered and snow-free winter imagery (December-March) and snow-free spring imagery (April-June). We found that using the snow-covered winter images suppressed

background spectral signatures and resulted in a higher overall classification accuracy of 93.7% for juniper densities above 15 percent, compared to snow-free winter imagery and spring imagery. When characterizing juniper densities below 10 percent our 30-meter pixel level classification map was unreliable, with an 11% probability of correctly classifying juniper. Therefore, we used Random Forests, a machine-learning algorithm, to develop a model of low-density (≤ 15%) juniper based on classified juniper cover and other ecological factors. We used the receiver operating characteristics (ROC) curve to evaluate model predictions; accuracy was high with an area under the curve (AUC) of 0.884. Our susceptibility map indicated that an additional 7.7% of the study area currently contained low densities of juniper and had high to very high risk of future encroachment. This study will provide agencies and land managers with information and techniques needed to address juniper encroachment in the Northern Great Plains.

CHAPTER 1

INTRODUCTION

The Great Plains has been recognized as North America's most endangered ecosystem (Samson and Knopf, 1996). A major concern has been the threat of converting grasslands to agriculture through cultivation practices (Sampson et al., 2004). However, woody plant encroachment should not be overlooked as it has already overwhelmed much of the southern Great Plains (Norris et al., 2001; Starks et al., 2014) and is spreading rapidly in the north (Meneguzzo and Liknes, 2015; Pierce and Reich, 2010). Encroaching and invasive species in the United States are an economic burden with environmental damages and losses totaling $120 billion per year (Pimentel et al., 2005). This cost will increase as eastern redcedar (*Juniperus virginiana)*, a single encroaching woody plant, was projected to cost the state of Oklahoma $447 million in economic losses for 2013 (Oklahoma Conservation Commission, 2008). Woody plant encroachment not only contributes to economic losses, but is threatening natural ecosystem functions as well. Hydrological processes are being altered through increases in soil infiltration and reduced streamflow (Zou et al., 2014; Zou et al., 2016), while carbon storage is shifted from belowground to aboveground (McKinley and Blair, 2008), and altered microclimates result in a change in plant communities to predominantly non-natives (Pierce and Reich 2010). Because of these impacts, grassland loss resulting from juniper encroachment can substantially affect the grassland industry by reducing livestock production up to 75 percent (Fuhlendorf et al. 2008). This is why it is important to monitor woody plant encroachment, yet there is a general lack of data sources

providing distribution estimates and site-specific information that is necessary for implementing the appropriate management measures.

Juniper Encroachment

Various species of woody plants such as *Prosopis* (mesquite), *Larrea* (chaparral), and *Juniperus* (juniper) are encroaching into the Great Plains at a high rate with little constraint giving the process the name, the *Green Glacier* (Engle et al., 2008; Van Auken, 2009). These native species were once restricted by fire but are now expanding into new u territories (Bragg and Hulbert 1976; Briggs et al., 2002a). A long history of fire suppression, land use changes, and a high rate of active planting are contributing to the expansion of juniper. Since the early 1930's, conservation programs have promoted the enhancement of shelterbelts and the preservation of wildlife habitat. In doing so, millions of eastern redcedar were planted (Knezevic, et al. 2005). Ganguli et al. (2008) reported that in 2001, nurseries within 20 states produced approximately 2.3 million eastern redcedar seedlings of which 80 percent were distributed within the Great Plains. Even today, many cost-share programs such as the Environmental Quality Incentives Program (EQIP) and Conservation Stewardship Program (CSP) provide financial assistance to private landowners who plant trees for wind protection, habitat improvement, and soil and water conservation (USDA-NRCS, 2017). Often, this includes the planting of juniper species such as Eastern redcedar as they are drought hardy and readily available (Ganguli et al., 2008). Activities such as the promotion of planting junipers only expedites the spread of juniper, as these programs do not take into account the invasive habits of the species (Roberts et al., 2018).

The eastern redcedar is a well-adapted species that persists under a variety of environmental and topographical conditions (Van Haverbeke & Read 1976). The fast spreading nature of juniper can be attributed to a high seed dispersal rate, its ability to quickly establish on poor soils, and its extreme tolerance for drought (Briggs et al. 2002a, Caterina et al. 2014). These factors allow eastern redcedars to outcompete dominant native species such as big bluestem (*Andropogon gerardii*; Axmann and Knapp 1993). These effective adaptations have allowed the juniper to succeed in the prairie ecosystem of the Great Plains.

Once the juniper is established the canopy density increases, ultimately affecting surrounding soil moisture, temperature, and light penetration (Pierce and Reich, 2010). This change in the microclimate surrounding the trees promotes the shift in species composition from dominant C4 grasses to non-native C3 grasses, such as *Poa pratensis,* and eventually results in low understory plant cover and species richness (Gehring, and Bragg, 1992). The entire process leads to an increase in juniper density and an overall loss in herbaceous biomass and reduction in rangeland productivity (Briggs et al., 2002a).

The rate at which juniper encroachment is affecting the Great Plains has been assessed through multiple studies. In the Flint Hills of Kansas, Briggs et al. (2002a) found that juniper expansion was occurring at a rate of 5.7 percent per year and eventually resulted in a closed-canopy forest within a 40-year timespan. In Oklahoma, Wang et al. (2017) calculated an annual encroachment rate of 8 percent between 1984 and 2010. Walker and Hoback (2007) observed a 2 percent annual expansion rate in central Nebraska. Similarly, Meneguzzo and Liknes (2015) observed Nebraska was losing 20,000 acres of non-forestland annually to juniper, giving Nebraska the highest

juniper conversion rate within the central United States. Regardless of the exact expansion rate, juniper is establishing within the Great Plains at an alarming pace. With this change, follows the damaging effects associated with an increasing area of established junipers.

Juniper Management

Management of encroaching juniper is vital when attempting to prevent any present or future ecological damages caused by the species. The implementation of juniper management occurs at two stages: proactive management and reactive management (Simonsen et al., 2015). Proactive management provides a lower human risk factor (i.e. less potential for human bodily and property harm) with less invasive management teqniques, while also being the most cost effective measure for controlling juniper (Wilson and Schmidt, 1990). This process consists of planning and implementing procedures before the establishment of juniper has occurred or when juniper is in a vulnerable seedling state. Some successful measures include high intensity goat grazing, haying, and low-intensity prescribed burning (Simonsen et al., 2015; Smith, 2011). When juniper is already established on the landscape and is in a dense to mature state, proactive management becomes less effective (Wilson and Schmidt, 1990). In response to already-established juniper, the implementation of reactive management measures is necessary. This type of management contains a higher human risk factor (i.e. greater potential for human bodily and property harm) as it entails intense management teqniques such as mechanical removal by timber cutting, herbicides, and intense prescribed burning (Simonsen et al., 2015; Smith, 2011; Wilson and Schmidt, 1990).

As juniper increases in size and stand density, the overall cost of managing and removing the juniper increases (Bidwell et al 2002; Ortmann el al., 1998). In 2002, the cost of executing a prescribed burn on non-to low cedar infested area of 160 to 640 acres was seven dollars per acre. For more mature, dense stands, the cost increased to roughly $25 per acre (Bidwell et al 2002). However as tree height increases, prescribed burning becomes an insufficient control method, as there is only a 35 percent mortality rate for junipers above two meters and 10 percent mortality rate for junipers above three meters (Buehring et al., 1971; Ortmann el al., 1998). Mechanical removal becomes the preferred method of control when trees become too tall for burning to be effective. Mechanical removal costs exceed those for prescribed burning. For the same 160 to 640 acres, implementing mechanical removal on juniper above two meters in height ranges from $40 to $90 per acre. Reactive management of juniper can be costly and time consuming. Therefore, proper planning for management is imperative in order to save on overall, financial and labor investments.

Juniper Inventory

The United States Department of Agriculture (USDA) Forest Service Forest Inventory and Analysis (FIA) program allows land managers and state agencies to obtain forest estimates for each state (USDA Forest Service, 2018). On a yearly basis, the FIA program measures 20 percent of their designated woodland plots within each state. This sampling method allows for a calculation of yearly tree attribute estimates and provides a statewide inventory every five years (Burkman, 2009). These tree inventory assessments

allow managers to retrieve repeated field measurements for evaluating forest resources and identify any changes to the overall forest condition (Meneguzzo and Liknes, 2015).

In 2012, Meneguzzo and Liknes (2015) used FIA data to show an eight state regional estimate of 894 thousand acres of juniper forestland. In 2016, Nebraska had an estimated 235 thousand acres of *Juniperus virginiana* whereas South Dakota had a combined juniper estimation (*Juniperus virginiana* and *Juniperus scopulorum*) of 124 thousand acres (Meneguzzo, 2017; Walters, 2017). This combined state total makes up 40 percent of the 2012 juniper acreage for the eight states located in the Midwestern United States. Meneguzzo and Liknes (2015) were also able to show that over a seven year time span (2005-2012) juniper forests increased by 287,000 acres in eight states. This resulted in an annual loss of 41,000 acres of non-forestland to juniper encroachment between 2007 and 2012.

The FIA provides quality statewide attribute estimates, though there are no mapping components provided through this platform. The combination of interpolation techniques, remotely sensed data, and FIA plots can provide visual representations of juniper on the landscape. This approach has been adopted by using MODIS (or Moderate Resolution Imaging Spectroradiometer; 250-meter pixel size) to produce low resolution live volume and density maps of juniper (Meneguzzo et al., 2008; Ruefenacht et al., 2008; Simonsen et al., 2015). Although these maps can identify general patterns over large areas at a low resolution, the attribute estimates and maps do not necessarily depict actual tree locations. The use of higher resolution data sources (e.g. Landsat; 30-meter pixel size) would allow for better visual assessments.

Juniper Mapping

Through the act of obtaining information about an object or phenomenon without having contact with that object or phenomenon, remote sensing becomes a useful tool for land cover classification and is commonly used in forest management (Franklin, 2001; Giri, 2012). Using remotely sensed images, managers can assess forest cover and stand health (Heilman et al., 2002; Wulder et al., 2006), and the resulting information can be used for implementing management decisions. Remote sensing of juniper encroachment provides land managers with useful distribution maps, quality estimates, and allows for the monitoring of site-specific areas. Based on the results of previous research, there are multiple data sources and methods that can be used for classification and mapping of juniper.

With very high spatial resolution (VHSR) aerial imagery (0.5 to 1-meter pixel size), studies have shown the ability of automated classification methods to classify individual junipers with high accuracy, but have also found that limitations as shadow effects can influence the detection of clustered trees (Anderson and Cobb, 2004; Poznanovic et al., 2014). Sources such as the National Agriculture Imagery Program (NAIP) can provide VHSR imagery at a 60 cm resolution for the agricultural growing season and are available on two to three year cycles (USDA Farm Service Agency, 2018). Another image source has included the use of VHSR hyperspectral data. Hyperspectral sources contain many spectral bands, which record information in narrow wavelength ranges for a more precise spectral separation between materials; allowing for the classification of species-specific vegetation. Wylie et al. (2000) was able to map woody and herbaceous vegetation, including eastern redcedar, using Airborne Visible

Infrared Imaging Spectrometer (AVIRIS), but was limited to a single flight and designated two by five kilometer flight path.

The opening of the Landsat archive, combined with easy-to-access products such as Landsat Analysis Ready Data (ARD), have made it possible to continuously monitor juniper. Since 1984, the Landsat program has provided 30-meter pixel size images at a 16-day temporal resolution (Wulder et al., 2016, Wulder et al., 2012). At a 30-meter medium resolution, classification of juniper is more successful when a pixel does not contain multiple cover types (Sankey and Germino, 2008). When multiple materials (e.g. different vegetation types) are within a single pixel, it can be difficult to correctly classify the intended material of interest (e.g. juniper), resulting in misclassifications of juniper sites as non-juniper and non-juniper sites as containing juniper.

The approach of fusing multiple data sources has allowed for a better representation of land cover characteristics when working within a diverse landscape. Sankey et al. (2010) were able to use the fusion of Landsat Thematic Mapper (TM) and Light Detection and Ranging (lidar) data to increase their juniper classification accuracy while retaining juniper cover information, though they were restricted to a 239 km^2 study area. A more recent study was able to show the capabilities of using multiple data sources to map juniper encroachment at a large extent, approximately 28,303 km^2. Wang et al. (2017) used a pixel and phenology-based mapping algorithm to analyze Landsat (TM/ETM +) and Advanced Land Observing Satellite (ALOS) Phased Array type L-band Synthetic Aperture Radar (PALSAR) in order to assess the dynamics of juniper encroachment over five historical time periods within a 30 year timeframe. The use of PALSAR allowed them to extract boundaries of forests that contained both coniferous

and deciduous trees while winter spectral values obtained from Landsat data during the winter allowed for the separation of tree types. Although they produced useful results, ALOS PALSAR stopped operation in 2011, preventing any future utilization of this data source. For management applications, there is a need for the ability to produce accurate juniper classification maps with replicable detailed classification methods that allow for the assessment of current and future juniper encroachment.

Objectives

To address these needs, we investigated the classification of two juniper species (*Juniperus virginiana* and *Juniperus scopulorum*; referred to as "juniper" hereafter) using a linear spectral unmixing method on Landsat 8 medium resolution satellite imagery and a predictive spatial model. We implemented a workflow for large-scale juniper mapping to 14 contiguous counties bordering the Missouri River in southeastern South Dakota and northeastern Nebraska for an approximate area of 23,000 km^2. Our objectives for this study were to:

1. Develop a practical workflow for large-scale juniper mapping using Landsat 8 Operational Land Imager (OLI) imagery and partial unmixing techniques.
2. Compare the classification accuracies from the resulting map based on different juniper density thresholds and different types of imagery.
3. Develop a predictive spatial model for the distribution of low-density juniper based on distance to seed source and environmental covariates and determine the prediction accuracy.

4. Use the resulting maps to evaluate the extent of current juniper establishment and the risk of future encroachment.

Research Questions

We asked the following major research question:

1. How does the use of winter versus non-winter imagery, and of snow-covered versus non snow-covered imagery, affect accuracy when classifying juniper?
2. What are the primary ecological predictors associated with the distribution of low-density juniper across the study area?
3. Which areas across the landscape are at high risk for future juniper encroachment?

CHAPTER 2

MAPPING JUNIPER ENCROACHMENT INTO A PRAIRIE LANDSCAPE

Abstract: Eastern redcedars (*Juniperus virginiana*) have been receiving considerable attention recently as their footprint significantly increases within the prairie ecosystems of the Great Plains. The encroachment of this species poses a threat to native habitats where it alters soil characteristics, limits undergrowth and herbaceous biomass, hinders native community regeneration, and negatively affects rangeland production. Management is vital to controlling juniper, yet there is a general lack of resources providing distribution estimates and site-specific information that is necessary for implementing the appropriate management measures at the appropriate scale. In this study, we evaluated the classification accuracy for juniper detection using a matched filtering technique with Landsat 8 OLI (Operational Land Imager) snow and non-snow covered winter imagery (January-March), and snow-free spring imagery (April – June) for 2015-2016. We developed a practical workflow for large-scale juniper mapping which we applied to two Landsat 8 path/rows (29/30 and 30/30) covering the counties bordering the Missouri River in southeastern South Dakota and northeastern Nebraska for an approximate area of 23,000 km^2. In both path/rows, we found that using snow-covered winter images suppressed background spectral signatures and resulted in higher overall classification accuracies of 94.5% and 88.9% for juniper densities above 15 percent, compared to 91.4% and 85.7% for non-snow covered winter imagery and 57.8% and

74.1% for spring imagery. For winter imagery, we successfully captured pixels containing juniper density above 50 percent with ≥ 90% detection probability. In images containing snow coverage, the juniper true positive rate significantly decreased once juniper densities fell below 20 percent, dropping to 48% and 37% respectively for path/rows 29/30 and 30/30. This study will allow for the continuous monitoring of juniper encroachment in the Upper Great Plains over a large scale while also assisting land managers in establishing and implementing the appropriate management measures.

Introduction

Juniper encroachment, particularly eastern redcedar (*Juniperus virginiana*,), has been receiving considerable attention recently as the distribution of this species significantly increases and threatens portions of the prairie ecosystems of the Great Plains. The spatial extent of juniper was once greatly restricted by fire, but is now expanding into new habitats (Briggs et al., 2002a; Twidwell et al., 2013). A long history of fire suppression, land use changes, and fluctuating environmental conditions have all contributed to the expansion of the eastern redcedar (Briggs et al., 2002a). The encroachment of this juniper species has the potential to alter native grasslands by changing soil characteristics, limiting undergrowth and herbaceous biomass, hindering native community regeneration, and affecting rangeland forage production (Briggs et al., 2002b; Gehring and Bragg, 1992; McKinley and Blair, 2008). In order to prevent the effects of juniper encroachment on grasslands, management practices such as mechanical removal, chemical application, and prescribed burning are utilized for control, serving as critical methods for prevention of population expansion (Wilson and Schmidt, 1990).

However, mechanical management of juniper by timber cutting or prescribed burning can be time consuming, costly, and ineffective; especially as tree size and stand density increases (Bidwell et al 2002; Buehring et al., 1971; Ortmann el al., 1998). Accurate distribution estimates and updated encroachment maps of juniper may aid in targeting susceptible areas for implementing proactive measures and defining appropriate management methods for established juniper woodlands, thus saving overall financial and labor investments.

Currently, land managers and state agencies access juniper estimates through the Forest Inventory and Analysis (FIA) program of the United States Department of Agriculture Forest Service (accessed at www.fia.fs.fed.us). The FIA program collects field data on a fraction of one-acre forestland plots within a state, allowing computation of yearly tree attribute estimates while providing a complete statewide inventory at five year intervals (Burkman, 2009). Meneguzzo and Liknes (2015) used this data to show that over a seven year time span (2005-2012) juniper forest increased by 287,000 acres in the central United States; this resulted in an annual loss of 41,000 acres of non-forestland to juniper encroachment between 2007 and 2012. The FIA data can provide estimates of juniper extent and can also be used to develop maps of juniper density. For example, the information collected through the FIA process has been combined with MODIS (or Moderate Resolution Imaging Spectroradiometer; 250-meter pixel size) imagery to interpolate and produce low-resolution live volume and density maps of juniper (Meneguzzo et al., 2008; Ruefenacht et al., 2008; Simonsen et al., 2015). Although these maps and area estimates are suitable for general assessments of juniper distribution over large areas, they do not necessarily depict actual tree locations. Additionally, as the area

of interest becomes smaller, the sampling error increases and the reliability of the data decreases (O'Connell et al. 2017).

As juniper continues to encroach into the grasslands of the Great Plains, higher resolution maps are needed to make accurate landscape-level assessments and site-specific management decisions. Remote sensing has been applied to generate maps and support these assessments, but mostly at relatively small spatial extents. Previous studies have incorporated very high spatial resolution (VHSR) aerial imagery (Anderson and Cobb, 2004; Poznanovic et al., 2014), hyperspectral data (Wylie et al., 2000), and multi-source fusion of Landsat Thematic Mapper (TM) and Light Detection and Ranging (lidar) data (Sankey et al., 2010). A more recent study has shown the potential for mapping eastern redcedar at a large scale with the combination of a long wavelength L-band Synthetic Aperture Radar (SAR) and Landsat Thematic Mapper/Enhanced Thematic Mapper Plus (TM/ETM +) (Wang et al., 2017). Although these studies have provided useful results, many of the data sources are temporally or spatially limited, making these approaches difficult to apply to other study areas.

Landsat provides a readily available data source that allows for the continuous monitoring of juniper. Since 1984, the Landsat program has provided 30-meter pixel size images at a 16-day temporal resolution (Wulder et al., 2012). Sankey and Germino (2008) used Landsat 5 (TM) imagery as single data source and a spectral mixture analysis to classify juniper in a 200 km^2 area. Though their methods are easily replicable, multiple materials within a single pixel can cause misclassification and lead to inconsistent results between spatially and temporally different scenes (Sankey et al., 2011). In order for juniper encroachment assessment to be applicable for management purposes, there is a

need for replicable classification methods that use readily available open source data to support continuous, high-accuracy mapping.

We investigated the classification of two juniper species (*Juniperus virginiana* and *Juniperus scopulorum*; referred to as "juniper" hereafter) in a prairie landscape using a linear spectral unmixing method on Landsat 8 medium resolution satellite imagery. Our objectives were to: 1) evaluate the classification accuracy for juniper detection using partial unmixing techniques with Landsat 8 OLI (Operational Land Imager) imagery; and 2) develop a practical workflow for large-scale juniper mapping. We assessed juniper detection at multiple densities and image conditions including: consistent snow coverage during the non-growing season, no snow coverage during the non-growing season, and imagery in the growing season. We then evaluated the replicability of the processes by applying the developed workflow to an additional path/row over temporally distinct timeframes and reporting the detailed pixel-level classification accuracy results.

Methods

Study Area

Our study area covers 14 contiguous counties bordering the Missouri River (nine counties in southeastern South Dakota and five counties in northeastern Nebraska; Figure 2-1). This area has a Köppen climate classification of humid continental (*Dfa*) (Kottek et. al., 2006), which is designated by an annual temperature range of 6-11 °C and an annual average precipitation of 498-796 mm (NOAA, 1981-2010). Common vegetation consists of mixed grass prairie species such as little bluestem (*Schizachyrium scoparium*), big bluestem (*Andropogon gerardii*), western wheatgrass (Pascopyrum smithii), sideoats

grama (*Bouteloua curtipendula*), and green needlegrass (*Nassella viridula*). Woodlands are primarily found near drainages and riparian lowlands, with the exception of small groves scattered across the prairie uplands. The most common deciduous species includes the plains cottonwood (*Populus deltoids*) with the occasional green ash (*Fraxinus pennsylvanica*) and American elm (*Ulmus americana*). Juniper species such as Rocky mountain juniper (*Juniperus scopulorum*) and eastern redcedar (*Juniperus virginianai*) are also common (Barker and Whitman, 1988). Steeply sloped drainages disrupt a flat to rolling topography comprised largely of agriculture (48%) and herbaceous grasslands (39%) producing a fragmented landscape. The primary land uses within our study area include the agricultural production of corn, soybeans, and wheat as well as cattle ranching.

Data Sources

We obtained a collection of Landsat 8 Operational Land Imager (OLI) Surface Reflectance level-2 imagery (path/rows 29/30 and 30/30; Figure 2-1) containing minimal cloud cover (< 10 percent) through the U.S. Geological Survey (USGS) EarthExplorer online tool (USGS Earth Explorer, 2017). Images obtained are generated from the Landsat Surface Reflectance Code (LaSRC). We investigated each image for anomalies (i.e. patches of greenness, cloud shadows) with the provided Level-2 Pixel Quality Band and selected three uniform images that covered the study area for each path/row. We selected images from two seasonal time periods, including two images from the non-growing season (January through March) as well as one image within the active growing season (April through July). For the non-growing season: we selected one image showing

consistent snow coverage and one containing no snow coverage for the study area. Once we selected appropriate dates, we then extracted the six bands: band 2 (0.435-0.451 µm, blue), band 3 (0.533-0.590 µm, green), band 4 (0.636-0.673 µm, red), band 5 (0.851-.0879 µm, near infrared), band 6 (1.566-1.651 µm, shortwave infrared), and band 7 (2.107-2.294 µm, shortwave infrared). Table 2-1 shows the final six images obtained for our analyses.

To reduce any spectral misclassification we constructed a mask for each image that subset the study area and excluded any water body features (i.e. streams, rivers, ponds and lakes). We identified water bodies using the USGS National Hydrography Dataset (NHD), obtained through Geospatial Data Gateway (NRCS, 2017). The mask was then used during the classification analyses.

Juniper Classification

We performed juniper classification using a matched filtering approach with ENVI version 5.4 (Exelis Visual Information Solutions, Boulder, Colorado). Matched filtering is a partial unmixing process that incorporates user-defined endmembers to maximize the response of known spectral indices while suppressing the unknown background indices. We performed this classification on each dataset by selecting a pure endmember, the selected bands within our image, and an image mask that corresponded with the chosen dataset.

Matched filtering requires only the input of the desired endmember or cover type that the user wishes to identify. This differs from conventional linear spectral unmixing (LSU) which requires an input of all known endmembers. Previous partial unmixing

research has indicated that the mean of manually selected endmembers containing a high percentage of target cover outperformed extreme or variant n-dimensional visualizer (ND-V) endmember pixels and the mean of all ND-V endmember pixels (Sankey and Glenn, 2011). Therefore, we selected ten pixels that were predominantly juniper within each path/row (29/30 and 30/30). This process allowed the average spectral signature to be obtained, which we used as the endmember input for our matched filtering analyses.

After selecting the endmember, we began assessing the stacked images for the optimal band combinations. Previous studies and preliminary observations suggested that a combination of bands 2-5 and band 7 allowed for the best spectral separation between juniper and background materials (Vikhamer and Solberg, 2002). We then generated a matched filtering image that contained values that represented the relative degree of match for each pixel. A value of one signified a perfect match while values closer to zero reflected background or non-target materials.

Once we completed the matched filtering analysis, we developed a binary juniper classification map by designating a threshold for the matched filtering values contained within the image. We determined a threshold for each image by sampling a group of user-defined pixels that contained a high percentage (>50 percent) of juniper cover. We then computed the mean Matched Filtering value and standard deviation for the sampled pixels and assigned two negative standard deviations from the mean as our threshold. We produced a final classification map that contained pixels representing juniper and non-juniper, with new values of one and zero.

Accuracy Assessment

To assess accuracy we used a random stratified sampling design for our study area that allowed us to determine the classification accuracy over a range of juniper densities. In doing so, we allocated four strata, which included closed canopy woodlands, buffered closed canopy woodlands, planted shelterbelts, and non-woodland areas. We digitized the closed canopy woodlands and planted shelterbelts in ArcGIS following the guidelines presented in (Bauman et al., 2016) using very high spatial resolution (VHSR) 60cm National Agricultural Imagery Program (NAIP), 2014 and 2016 aerial imagery. In addition to obtaining samples of dense woodland cover, we sought to capture less dense samples of open canopied and sporadic trees. To do so, we placed a 90-meter buffer around our digitized closed canopy stratum in ArcGIS 10.5; from visual observations, we determined this to be an appropriate distance to capture additional low-density juniper.

Once we defined all the strata within the study area, we generated random points within ArcGIS 10.5. We then referenced each random point to a Landsat pixel by converting each point to a 30x30 meter polygon and snapping them to the Landsat 8 pixel grid. Thereafter, we characterized each polygon using a combination of VHSR imagery, which included NAIP 2016 and other sources of winter imagery accessed through Google Earth from 2013-2017 (Figure 2-5). Each sample delineation included the recording of the land cover type, juniper presence/absence, and the percent of juniper cover within the 30x30 meter polygon. We delineated 1,643 juniper presence and 2,273 juniper absence points for the assessment of classification accuracy at different juniper densities (Figure 2-2).

Field Investigation

We conducted field investigations during October 2017 to obtain ground reference data and gain a better understanding of juniper distribution over our study area. Preceding the field investigations, we subset the study area by road accessibility and generated 205 random points in ArcGIS 10.5 (ESRI, Inc., Redlands CA). We designated the random points as investigation sites where we conducted a 0.5 kilometer driven transect. Each transect was divided into three stops, and again each stop was divided into a left and right side (six stops per transect). At each stop, we captured a photo with a GPS enabled digital camera and recorded vegetation and land cover characteristics (e.g. land use, species composition). We also took additional photos at opportunistic stops. Similar field census methods were used in (Hutcheson and Rothe, 1977). We collected data for 252 sites and obtained 1271 photos distributed throughout our study area (Figure 2-2).

Results

We produced a total of six Landsat 8 juniper classification maps under three image conditions (consistent snow coverage during the non-growing season, no snow coverage during the non-growing season, and growing season) for two path/rows: 29/30 and 30/30. Classification maps identified both non-juniper and junipers sites. A visual assessment using VHSR imagery and field investigation images found a reasonably accurate representation of juniper for all images in the non-growing season (Figure 2-3a, b). However, misclassification of non-juniper (i.e. cultivated fields and wetlands) as juniper was observed more frequently in images containing no snow coverage (Figure 2-3a) than it was in images containing consistent snow coverage (Figure 2-3b).

Classification maps for the growing season appeared to have a high misrepresentation of both juniper and non-juniper sites (Figure 2-3c), which was confirmed during the accuracy assessments.

The matched filtering classification of images containing consistent snow coverage during the non-growing season allowed for the best separation of juniper and non-juniper and produced the most accurate maps in both path/rows (29/30 and 30/30) when juniper density was greater than 15 percent. Accuracy assessments for all six juniper classification maps is shown in Table 2-2. We obtained overall accuracy (OA) of 94.5% and 88.9% for path/rows: 29/30 and 30/30 compared to non-snow coverage during the non-growing season (91.4% and 85.7%) and growing season (57.8% and 74.1%). Our accuracy assessment for the juniper class indicated that higher producer accuracies (PA; the probability that a reference pixel of juniper is correctly classified) were achieved during the growing season of 92.1% and 84.7% compared to consistent snow coverage during the non-growing season (83.2% and 76.3%) and no snow coverage during the non-growing season (70.9% and 70.0%). However, both growing season images had significantly lower user accuracies (UA; the probability that a pixel classified as juniper actually represents juniper in the reference dataset) of 38.7% and 67.4% compared to consistent snow coverage during the non-growing season (96.3% and 99.2%) and no snow coverage during the non-growing season (96.8% and 98.3%).

The effectiveness of pixel-level matched filtering classification of juniper for non-growing season imagery was assessed at ten different juniper density groups (Figure 2-4). Quantitative pixel-level classifications for images in the active growing season were not assessed due to their low user accuracies and the visual unreliability of the output maps

(Figure 2-3c). True positive rate of juniper for both image conditions (Figure 2-4a, b) in the non-growing season was approximately 90% or higher for pixels containing juniper density above 50 percent (Figure 2-5f-j). Once juniper density dropped below 50 percent, the true positive rate varied more between each path/row and scene condition than that of pixels containing higher densities of juniper. The true positive rate for juniper dropped below 50% for images containing no snow coverage before that of imagery containing consistent snow coverage during the non-growing season (Figure 2-4a, b). This occurred for non-snow covered images when juniper densities were at 20-30 percent (Figure 2-5c; path/row: 29/30 and 30/30; 47% and 40%) and at 10-20 percent (Figure 2-5b; 48% and 37%) when images contained constant snow coverage during the non-growing season. Once juniper in pixels became more sporadic or dispersed at a 1-10 percent density (Figure 2-5a), the true positive rate was minimal, having a < 13% probability of detection for all images.

A final Landsat juniper classification map was created by overlaying the juniper classification maps produced from snow-covered imagery in path/row: 29/30 and 30/30. Our classification map, shown in Figure 2-6a, captures planted juniper while also detecting areas of spreading juniper (Figure 2-6b, c). The final classification map also shows the capability of the matched filtering technique in separating juniper from surrounding deciduous woodlands (Figure 2-6d, e). Pixels with intermixed woodlands (deciduous and juniper) were also classified as containing juniper.

Discussion

Our visual and quantitative accuracy assessments support the use of partial unmixing techniques with Landsat 8 OLI imagery that contains consistent snow coverage during the non-growing season for mapping juniper. Our classified maps attained higher overall classification accuracies when imagery in the non-growing season was used. Our use of a single data source and partial unmixing methods allowed us to obtain comparable juniper classification results to that of methods using multi-source data (Sankey et al., 2010; Wang et al., 2017) and hyperspectral data (Wylie et al., 2000). When images of the non-growing season were used, we successfully captured pixels containing juniper density above 50 percent with a 90% and greater detection probability, and we also obtained a true positive rate of 50% or greater for pixels containing juniper density above 15 percent. These quantitative pixel-level classification results are comparable to Wang et al. (2017) who saw a 90% detection probability for pixels containing eastern redcedar (*Juniperus virginiana*) density above 60 percent and a 30% detection probability when pixel densities where between 10 to 20 percent. This study ultimately allowed us to efficiently map juniper over a large spatial scale with the use of single source data that is readily available and analysis-ready (e.g. Landsat Level-1 and Level-2 data) when other data sources and methods were inapplicable.

Our pixel-level accuracy assessments depicted a distinctly occurring trend. As the overall juniper density decreased within a pixel so did the probability of correctly classifying that pixel as containing juniper. Yet, the probability of correctly classifying a pixel as containing juniper remained high for pixels containing an increased level of juniper density. This observation can also be noted in the recent study of Wang et al.

(2017), where they suspected the unrecognition of pixels was influenced by juniper height and the omission of woodlands that did not meet their definition of a forest. However, in this study the loss of accuracy for low-density juniper (i.e. < 20 percent) can be attributed to the threshold we set after our match filtering classification. If the threshold is decreased the probability of positively identifying lower density pixels would increase, but at the expense of increasing the classification of non-juniper sites as juniper (i.e. false positives). Low-density juniper can be positively associated with an increase in vegetation and background heterogeneity where as an increase in juniper density results in lower background vegetation (Briggs et al., 2002b; Gehring and Bragg, 1992). This may influence the partial spectral unmixing classification as more non-juniper spectral signatures mask the spectral signatures of junipers within the pixel.

Our Landsat juniper classification maps produced higher overall classification accuracies for images during the non-growing season compared to images obtained during the growing season. This can be attributed to smaller differences in spectral signatures between juniper and other types of vegetation and woodlands during the growing season in comparison to the winter months, when juniper was the only green vegetation (Wang et al., 2017). We were also able to obtain a better spectral separation of juniper and non-juniper when images containing consistent snow coverage were used compared to images containing no snow coverage during the non- growing season. The snow covered pixels contained higher reflectance values in the visible wavelengths and near-infrared wavelengths (Dozier and Painter, 2004; Vikhamar and Solberg, 2003). This was almost contrary to the reflectance values of juniper, which were lower in the visible wavelengths and near-infrared wavelengths in comparison to that of the snow covered

pixels. This circumstance allowed us to obtain better spectral separation of juniper and non-juniper. We also suspected the snow cover aided in the classification of juniper by reducing variation in the background non-juniper matrix, permitting our material of interest (i.e. juniper) to be the primary driver of the scene covariance (Boardman et al., 1995).

The workflow developed in this study will allow for the assessment of juniper encroachment at a landscape level while facilitating regional reassessment of management polices (Roberts et al., 2018). Juniper encroachment maps aid in the monitoring of site-specific areas, allowing for the allocation of appropriate management decisions for protection of future grassland loss (Bauman et al., 2016; Wimberly et al., 2018). Our juniper classification data and maps will establish a baseline for future studies. Although this study focused on only two Landsat path/rows and a single date, our partial unmixing techniques of moderate resolution imagery can be applied at a larger extent and/or over extended durations. The use of remote sensing to address the dynamic encroachment of juniper at a large scale has only recently been investigated in the southern Great Plains (Wang et al., 2017; Wang et al., 2018), but is yet to be explored in the northern Great Plains. With a better understanding of the drivers associated with juniper encroachment, current ecological knowledge (Briggs et al., 2002b; Pierce and Reich, 2010), and the use of accurate juniper maps, we can manage encroaching juniper species more efficiently by promoting proactive management procedures while focusing on future encroachment susceptibility (Greene and Knox, 2014).

While our study focuses primarily on mapping juniper encroachment in a portion of the northern Great Plains, woody plant encroachment is threatening other North

American grassland communities (Knapp et al., 2008; Ratajczak et al., 2012; Van Auken, 2009). Accurate and timely data on the distribution of woody plant encroachment is essential for assessing the economic and ecological impacts of woody encroachment (Anadón et al., 2014; Zavaleta, 2000) and will assist in establishing and implementing the appropriate management measures (Bidwell et al., 2002; Ortmann et al., 2007; Smith, 2011). Juniper species were notably the fundamental woody plant threatening grassland habitats in our region (Engle et al., 2008). We were able to develop maps that accurately depict the distribution of juniper by using partial unmixing techniques of Landsat 8 OLI imagery. Our practical workflow will allow for the continuous monitoring of juniper encroachment over a large scale while allowing managers to focus on sensitive or site-specific areas.

Figures

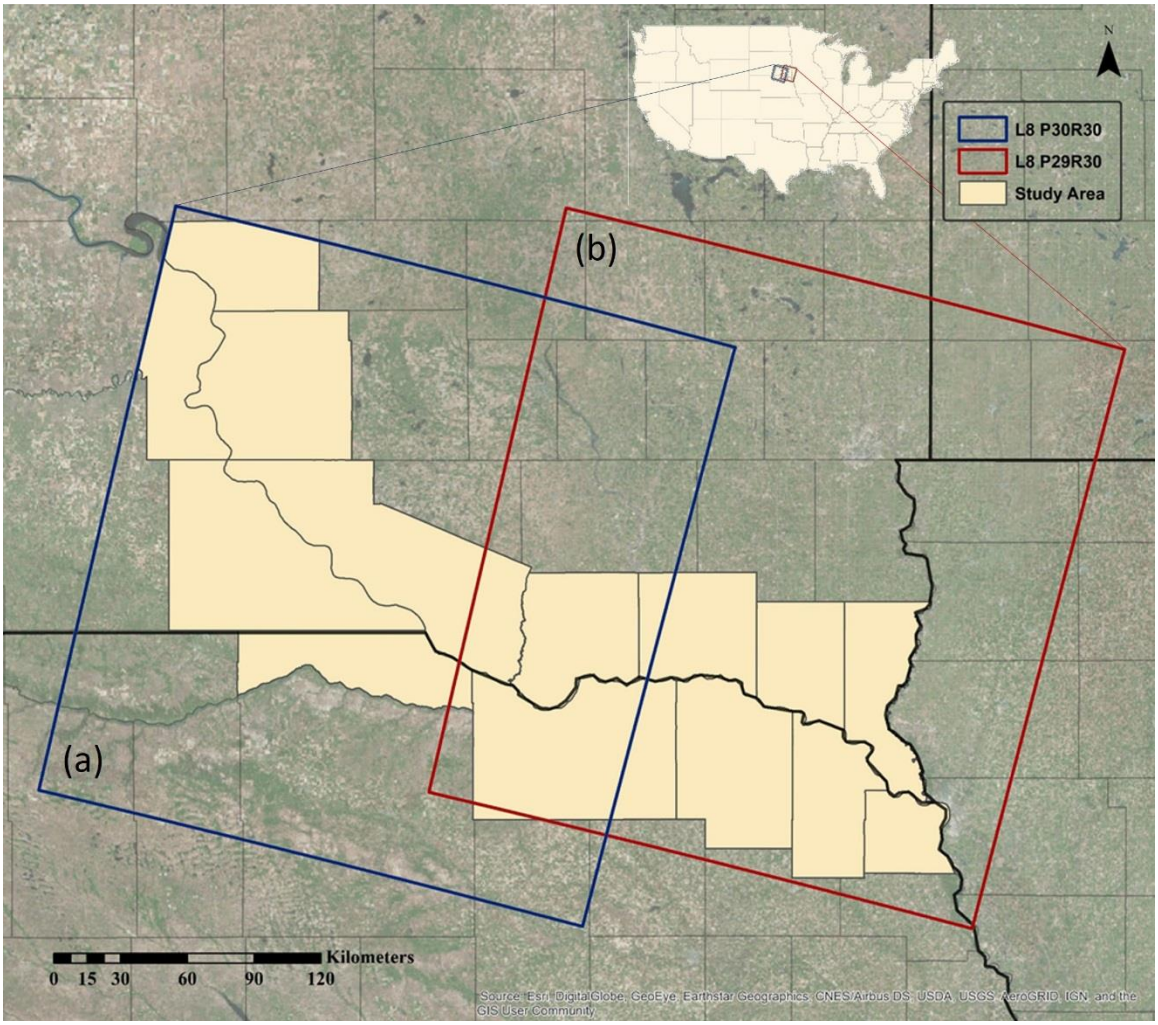

Figure 2-1. Study area composed of nine counties in southeastern South Dakota and five counties in northeastern Nebraska. Landsat 8 OLI path/rows: 30/30 (a) and 29/30 (b) cover the 14 contiguous counties.

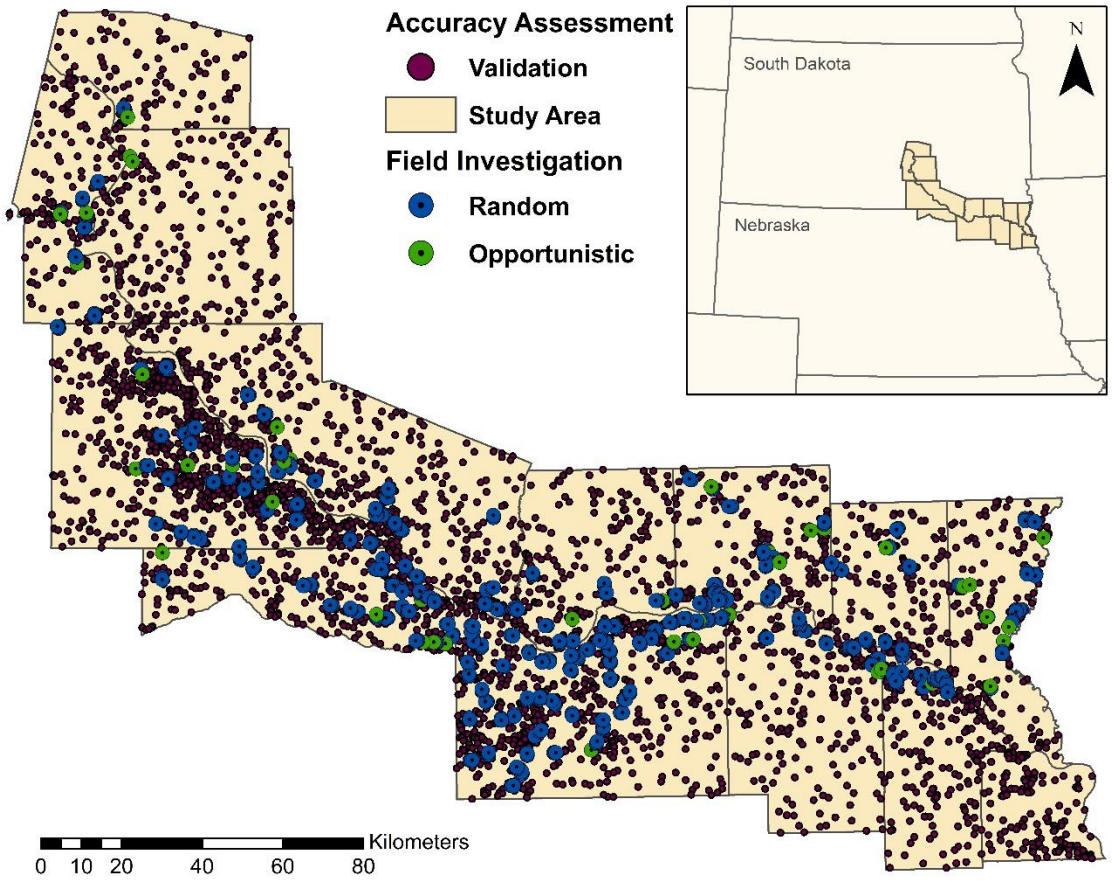

Figure 2-2. Visually interpreted juniper presence and juniper absence pixels for classification accuracy assessment along with field investigation sites.

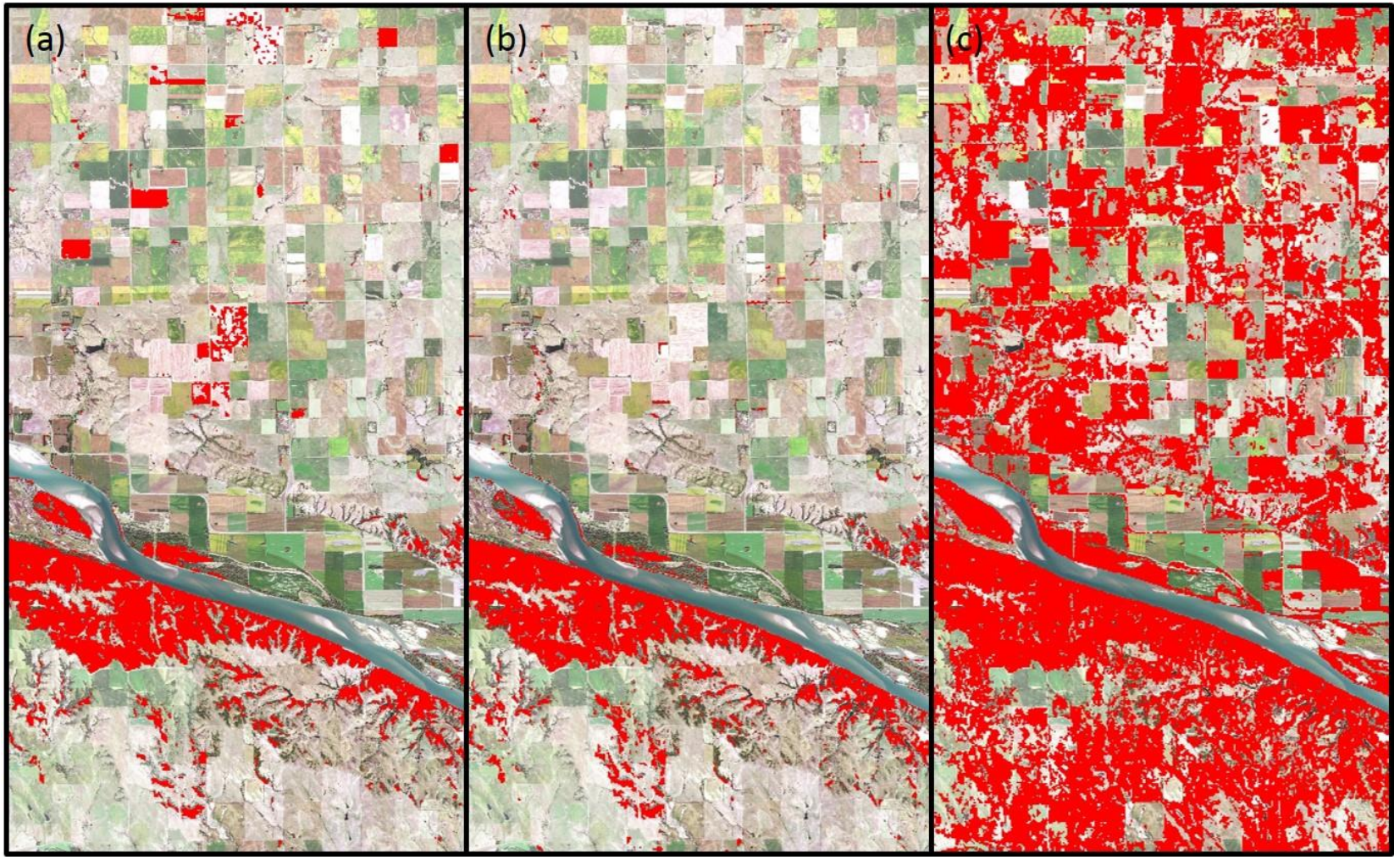

Figure 2-3. Qualitative assessment of juniper classification maps produced by Landsat 8 imagery during the non-growing season containing no snow coverage (a) and consistent snow coverage (b), and during growing season. Pixels classified as juniper maps are displayed over 2016 NAIP imagery.

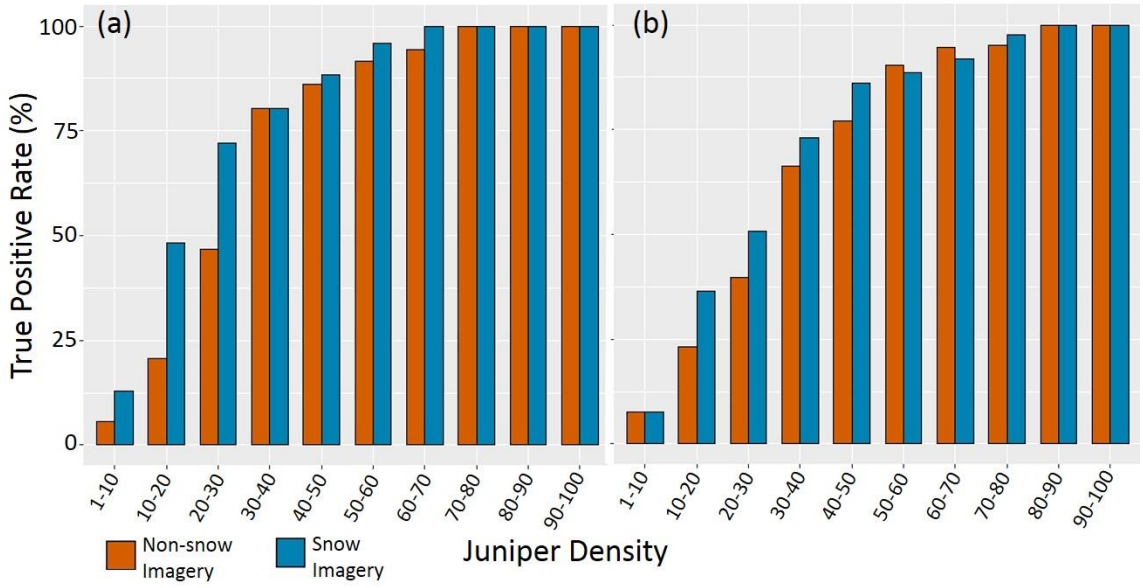

Figure 2-4. Pixel-level quality assessment for the classification of juniper by density with non-growing season imagery. Path/row: (a) 29/30 and (b) 30/30.

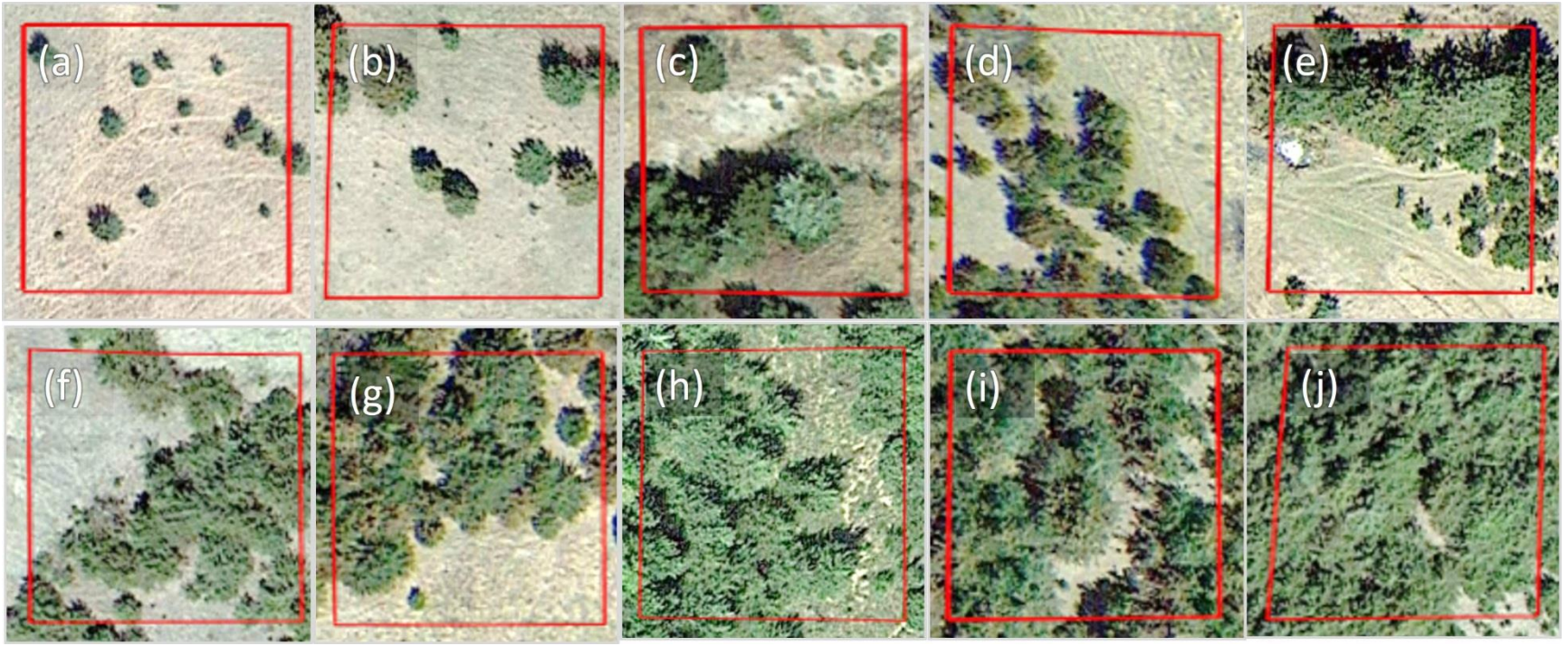

Figure 2-5. Examples of juniper density at 1-10 (a), 10-20 (b), 20-30(c), 30-40 (d), 40-50 (e), 50-60 (f), 60-70 (g), 70-80 (h), 80-90 (i), and 90-100 percent (j). 30 x 30 meter polygons are layered over NAIP and Google Earth imagery.

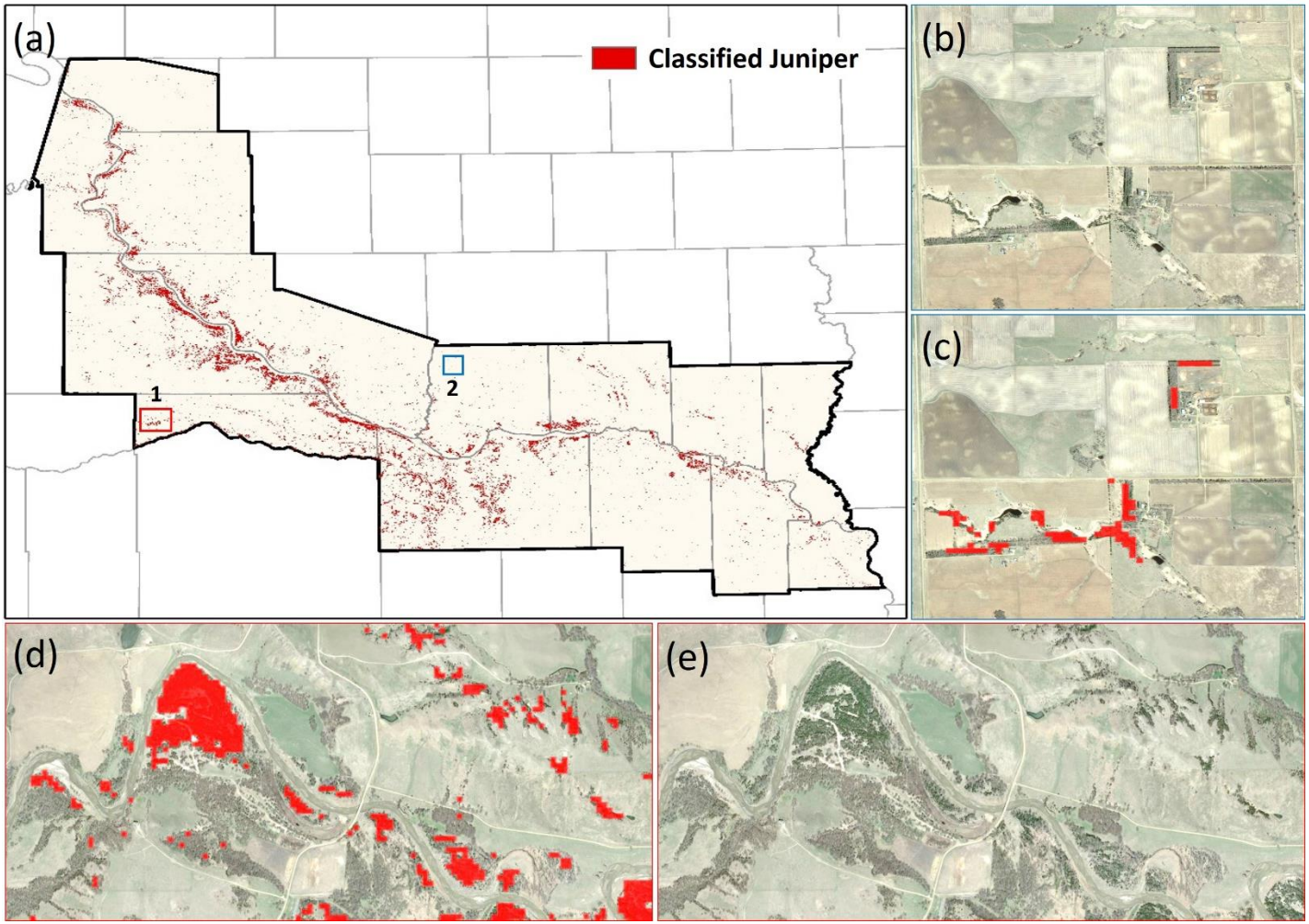

Figure 2-6. Final juniper classification map (a) showing close-up views (b-e) of regions 1, 2 in (a). (b, c) show juniper spreading from planted shelterbelts. (d, e) show juniper separation from deciduous woodlands. A Google Earth image dated 4/11/2016 shows junipers as green while leaf off deciduous trees remain brown.

Tables

Table 2-1. Landsat 8 OLI Surface Reflectance Level-2 imagery used for the classification of juniper. Cloud cover and snow cover represent the percent of the scene covered by either cloud or snow/ice.

Product Identifier	Date	Path/row	Cloud cover	Snow cover
LC08_L1TP_029030_20150107_20170302_01_T2	2015/01/07	29/30	1.55	94.75
LC08_L1TP_029030_20150328_20170227_01_T1	2015/03/28	29/30	1.11	0.00
LC08_L1TP_029030_20160602_20170223_01_T1	2016/06/02	29/30	7.41	0.00
LC08_L1TP_030030_20160101_20180131_01_T1	2016/01/01	30/30	0.05	97.91
LC08_L1TP_030030_20160305_20170224_01_T1	2016/03/05	30/30	0.45	0.00
LC08_L1TP_030030_20160524_20180131_01_T1	2016/05/24	30/30	0.00	0.00

Table 2-2. Accuracy assessment of six juniper classification maps based on classified juniper presence and juniper absence pixels. Assessments are evaluated using all juniper densities greater than 15 percent. Shown underlined, overall accuracy (OA) represents the total classification accuracy for both juniper presence and juniper absence pixels.

Path/Row	Condition	Classified pixel data	Reference pixel data			User Accuracy (UA)
			Juniper absence	Juniper presence	Row totals	
29/30	Snow	Juniper absence	887	57	944	0.9396
		Juniper presence	11	283	294	0.9626
		Column totals	898	340	1238	
		Producer accuracy (PA)	0.9878	0.8324		0.9101
29/30	Non-snow	Juniper absence	890	99	989	0.8999
		Juniper presence	8	241	249	0.9679
		Column totals	898	340	1238	
		Producer accuracy (PA)	0.9911	0.7088		0.8500
29/30	Growing	Juniper absence	403	27	430	0.9372
		Juniper presence	495	313	808	0.3874
		Column totals	898	340	1238	
		Producer accuracy (PA)	0.4488	0.9206		0.6847
30/30	Snow	Juniper absence	978	198	1176	0.8316
		Juniper presence	5	639	644	0.9922
		Column totals	983	837	1820	
		Producer accuracy (PA)	0.9949	0.7634		0.8792
30/30	Non-snow	Juniper absence	973	251	1224	0.7949
		Juniper presence	10	586	596	0.9832
		Column totals	983	837	1820	
		Producer accuracy (PA)	0.9898	0.7001		0.8450
30/30	Growing	Juniper absence	640	128	768	0.8333
		Juniper presence	343	709	1052	0.6740
		Column totals	983	837	1820	
		Producer accuracy (PA)	0.6511	0.8471		0.7491

CHAPTER 3

RISK ASSESSMENT OF JUNIPER WITH THE USE OF SUSCEPTIBILITY AND CLASSIFICATION MAPS

Abstract: The eastern redcedar (*Juniperus virginiana*), a widespread native juniper species, has become an ecological and economic burden on the prairie ecosystems of the Great Plains. The encroachment of this woody plant reduces rangeland production by decreasing herbaceous biomass and affecting natural ecosystem functions as it alters native plant communities, microclimates, and soil characteristics. Accurate distribution maps of juniper and predictions of areas at risk for future expansion are needed to support proactive management measures. Therefore, our objectives were to: 1) evaluate the pixel-level classification accuracy of remotely sensed juniper maps, 2) model the distribution of low-density juniper and determine the prediction accuracy, and 3) assign juniper susceptibility indices over a large-scale assessment site. The study area included counties bordering the Missouri River across southeastern South Dakota and northeastern Nebraska covering an approximate area of 23,000 km^2. We used a matched filtering technique with Landsat 8 Operational Land Imager snow-covered winter imagery (January-March) to classify juniper. Snow-covered winter images suppressed background spectral signatures and resulted in an overall classification accuracy of 94% when juniper densities were above 15 percent. We observed a decrease in the probability of characterizing juniper when densities within the pixel were below 20 percent. When

juniper densities were below 10 percent characterizing juniper at the 30-meter pixel level was minimal as there was only an 11% probability of correctly classifying juniper. To better identify areas with low-density juniper cover, we developed a model of low-density juniper with Random Forests based on environmental variables and distance to seed sources for mapping areas where future encroachment is likely. Model accuracy was high with an area under the curve (AUC) of 0.884. Results indicated that distance to nearest seed source and an abundance of surrounding juniper were the most important predictors. This study will provide agencies and land managers with information needed to address juniper encroachment in the northern Great Plains and with methods to expand the mapping project to new areas.

Introduction

Expansion of woody plants has threatened the natural ecosystem functions of North American grasslands (Knapp et al., 2008; Ratajczak et al., 2012; Van Auken, 2009). Notably the eastern redcedar (*Juniperus virginiana*), a prevalent juniper species, has affected carbon storage, soil characteristics, and plant communities within the prairie ecosystem of the Great Plains (McKinley and Blair, 2008; Norris et al., 2001; Pierce and Reich, 2010). In the central United States, juniper encroachment has resulted in a loss of 205,000 acres of non-forestland between 2007 and 2012 (Meneguzzo and Liknes, 2015). These changes have not only had an ecological impact but also has been damaging economically (Anadón et al., 2014; Yokomizo et al., 2009; Zavaleta, 2000). Increasing encroachment limits vegetation undergrowth and herbaceous biomass; hindering rangeland forage production (Briggs et al., 2002b; Gehring and Bragg, 1992). Simonsen

et al. (2015) reported that ranchers could see up to a 75% decline in forage resulting in an 80% decline in their returns due to eastern redcedar encroachment (Fuhlendorf et al., 2008; Ortman et al., 1998). Oklahoma State University (OSU) had projected a total economic loss of $447 million for the state in 2013 (Oklahoma Conservation Commission, 2008). The economic and ecological consequences of juniper encroachment will continue to increase unless preventative measures are implemented.

Management of encroaching woody plants is crucial especially when attempting to control a quickly expanding juniper footprint. Proactive and reactive management are two approaches for controlling juniper (Simonsen et al., 2015). Proactive management measures are implemented before the junipers have established or are in a vulnerable seedling state and consist of high intensity goat grazing, haying, or low-intensity prescribed burning (Simonsen et al., 2015; Smith, 2011; Wilson and Schmidt, 1990). On the other hand, reactive management practices are implemented in response to an already encroached landscape. Mechanical removal by timber cutting, herbicides, and intense prescribed burning are methods commonly utilized for controlling established juniper sites (Simonsen et al., 2015; Smith, 2011; Wilson and Schmidt, 1990). Reactive management of juniper is costly, time consuming, and may become ineffective as stand density and tree size increase (Bidwell et al 2002; Buehring et al., 1971; Ortmann el al., 1998). Therefore, proper planning is essential for using the most efficient management methods in a timely manner to save financial and labor investments.

Present-day juniper maps can aid in targeting areas for proactive management procedures, and accurate distributions allow for quality assessments of established juniper sites. Remote sensing is a common way of obtaining useful information

pertaining to forest stand condition that can be applied for management purposes (Franklin, 2001; Giri, 2012). Recently, juniper encroachment has been investigated with multiple data sources including very high spatial resolution (VHSR), aerial imagery (Anderson and Cobb, 2004; Poznanovic et al., 2014), hyperspectral data (Wylie et al., 2000), multispectral data (Sankey and Germino, 2008), and multi-source fusion of active sensors and multispectral data (Sankey et al., 2010; Wang et al., 2017). Although the results from these studies are useful, the data sources and methods are often spatially limited. In addition, there is a general lack of understanding as to the minimum juniper sizes and densities that can be identified by the classification methods. Wang et al. (2017) has explored this question over a large extent and observed within their designated assessment sites, a loss in juniper recognition when tree densities decreased below 20 percent. For management implications, it is necessary to consistently produce accurate juniper classification maps and to know the characteristics of the trees that can be consistently mapped.

As with most invasive species, the management of juniper for either economic or ecological objectives is best carried out during the early stages or even before encroachment has begun (Simberloff, 2003; Yokomizo et al., 2009). However, remotely detecting low-density juniper stands may become more difficult once the spatial resolution of the data source becomes coarser (i.e. 60cm VHSR to 30m Landsat). Alternatively, maps of juniper susceptibility can supplement juniper encroachment maps by representing areas at risk of low-density juniper encroachment. Greene and Knox (2014), predicted areas susceptible to juniper encroachment within a riparian setting and observed eastern redcedar was more likely to encroach higher energy depositional

surfaces containing sandy soils and a lower density of deciduous trees. However, this study was conducted in only one of the many habitats for redcedar (Lawson, 1990; Noble, 1990), and larger scale predictive models are needed for more broader application.

We investigated the classification of two juniper species (*Juniperus virginiana* and *Juniperus scopulorum*; referred to as "juniper" hereafter) with the intent of mapping low-density juniper susceptibility indices in a mixed landscape. Our objectives were to: 1) evaluate the pixel-level classification accuracy for juniper detection using partial unmixing techniques with Landsat 8 OLI (Operational Land Imager) imagery, 2) model the distribution of low-density juniper and determine the prediction accuracy based on distance to seed source and environmental covariates, and 3) assign juniper susceptibility indices over a large-scale assessment site.

Methods

Study Area

Our study area covered 14 contiguous counties (nine counties in southeastern South Dakota and five counties in northeastern Nebraska; Figure 3-1) all bordering the Missouri River. This area has a Köppen climate classification of humid continental (*Dfa*) (Kottek et. al., 2006), which is designated by an annual temperature range of 6-11 °C and an annual average precipitation of 498-796 mm (NOAA, 1981-2010). Common vegetation consists of mixed grass prairie species such as little bluestem (*Schizachyrium scoparium*), big bluestem (*Andropogon gerardii*), western wheatgrass (*Pascopyrum smithii*), sideoats grama (*Bouteloua curtipendula*), and green needlegrass (*Nassella viridula*). Woodlands are primarily found near drainages and riparian lowlands with the

exception of small groves scattered across the prairie uplands. The most common deciduous species includes the plains cottonwood (*Populus deltoids*) with the occasional green ash (*Fraxinus pennsylvanica*) and American elm (*Ulmus americana*). Juniper species such as Rocky mountain juniper (*Juniperus scopulorum*) and eastern redcedar (*Juniperus virginianai*) are also common (Barker and Whitman, 1988). Steeply sloped drainages disrupt a flat to rolling topography comprised largely of agriculture (48%) and herbaceous grasslands (39%) producing a fragmented landscape. Primary land uses within our study area include the agricultural production of corn, soybeans, and wheat as well as cattle ranching.

Data Sources

We used multiple data sources to extract predictor variables for our low-density juniper susceptibility analysis. We used the National Elevation Dataset (NED) with 30-meter spatial resolution to derive topographical factors. The NED is created by United States Geological Survey (USGS) and was accessed through the US Department of Agriculture (USDA) Geospatial Data Gateway (NRCS, 2017).

We used the gridded Soil Survey Geographic (gSSURGO) database obtained through the Geospatial Data Gateway to extract multiple soil characteristics. Gridded SSURGO contains the same data provided in the standard United States Department of Agriculture Natural Resources Conservation Service (USDA-NRCS) Soil Survey Geographic (SSURGO) database but is formatted as a Environmental Systems Research Institute, Inc. (ESRI) file geodatabase and is represented in a 10 meter spatial resolution raster format.

We obtained 30-year normals (1981-2010) of climatic factors including average annual minimum temperature (C°), average annual maximum temperature (C°), and average annual precipitation (cm) from the Parameter-elevation Relationships on Independent Slopes Model (PRISM) data. PRISM is based on an interpolation model that produces approximately four kilometer spatial resolution interpolations of annual climatic parameters using data from meteorological stations and a digital elevation model (DEM). The PRISM model is originated by the PRISM Climate Group of Oregon State University and can be accessed through the PRISM website (PRISM Climate Group, 2017).

We retrieved land cover data at a 30-meter spatial resolution from the 2016 Cropland Data Layer (CDL). CDL is generated by the Department of Agriculture, National Agricultural Statistics Service (NASS) and can be accessed through the CropScape portal (USDA-NASS Cropland Data Layer, 2016). We identified surface water features using the USGS National Hydrography Dataset (NHD). NHD is provided at a scale of 1:24,000 by the United States Geologic Survey (USGS) and can be accessed through the National Map Download viewer (USGS NHD, 2017). We obtained Landsat 8 Operational Land Imager (OLI) Surface Reflectance level-2 imagery (path/rows 29/30 and 30/30) from January 2015 to July 2016. Images are provided at a 30-meter spatial resolution with minimal cloud cover (< 10 percent) through the Earth Explorer portal (USGS Earth Explorer, 2017).

Juniper Classification

We produced a juniper classification map following the workflow described in Chapter 2 of this thesis. We began with obtaining a Landsat 8 image for each path/row: 29/30 and 30/30 (Figure 3-1), that contained consistent snow cover for the study area (Table 3-1). We performed the juniper classification using a matched filtering approach in ENVI version 5.4 software (Exelis Visual Information Solutions, Boulder, Colorado). Two matched filtering images were produced, which we then converted to binary juniper classification maps by designating a threshold for the matched filtering values contained within each image. We determined a threshold by sampling a group of user-defined pixels that contained juniper and computed the mean matched filtering value and standard deviation. Our threshold was then defined as being two standard deviations below the mean, which generated two binary outputs. The two binary outputs were merged in ArcGIS 10.5 (ESRI, Inc., Redlands CA) to create a final Landsat juniper classification map that contained pixels representing juniper and non-juniper.

Ecological Predictor Variables

Previous research has suggested multiple environmental conditions that are associated with juniper habitats. We examined 15 predictor variables shown in Table 3-2 that were hypothesized to be associated with juniper encroachment. These factors included percent slope, aspect, mean annual temperature, total annual precipitation, percent sand, percent silt, percent clay, soil available water storage, depth to restricted layer, root zone depth, soil drainage class, percent agriculture, distance to juniper, percent juniper, and distance to surface water. We processed these variables in ArcGIS 10.5 by converting or resampling to a 30-meter spatial resolution raster.

We used the NED to derive topographical variables. Percent slope represented the gradient of the physical landscape (Anderson, 2003). We also used aspect to indicate the direction the slope faced (Lawson, 1990; Schmidt and Stubbendieck, 1993). We reclassified aspect into nine categories including flat (zero percent slope), cardinal directions (N, E, S, W), and ordinal directions (NE, SE, SW, NW).

We used the PRISM dataset to extract climatic variables. We used the mean minimum temperature and mean maximum temperature of each pixel to derive the mean annual temperature (Anderson, 2003). We than created a precipitation map for the study area with values representing total annual precipitation (Owensby et al., 1973).

We used the gSSURGO database to derive soil characteristics. Soil texture is represented as three separate factors including percent sand, percent silt, and percent clay (Wang et al., 2018). A combination of these three factors can be used to define the soil classification within the soil profile (Anderson, 2003). We used the available water storage estimate (AWS) which represented the volume (mm) of plant available water the soil can store within a 0-150 cm soil profile (Wang et al., 2018). We used depth to restricted layer as a measure in the distance (cm) within the soil profile showing any restricting features that may constrain root growth or the movement of water and air. We used the root zone depth as a measure to the depth at which plants root systems can effectively obtain nutrients and water. We also extracted soil drainage class, which is characterized into seven classes (excessively drained to very poorly drained) and reflects the natural frequency and duration of wet periods for the soil (Soil Science Division Staff, 2017).

We used the 2016 CDL dataset to extract the percent agriculture within a five by five-pixel window surrounding an individual 30-meter pixel. The CDL is an annually produced raster, which has been georeferenced and contains crop-specific land cover data. We denoted agriculture as any human use of the landscape for cultivated crops, haying, and/or alfalfa fields.

We used our Landsat juniper classification map to generate two juniper conditioning factors. We used the Euclidean distance tool in ArcGIS 10.5 to create a conditioning raster where each pixel was the Euclidean distance to the closest juniper source (Bragg and Hulbert, 1976). We also used our Landsat juniper classification map to determine the percent juniper within a five by five pixel window.

We used the National Hydrography Dataset (NHD) to map the distance to the nearest surface water (Holthuijzen and Sharik, 1985). We used the Euclidean distance tool to create a raster where each pixel value was the Euclidean distance to the closest surface water feature.

Juniper Training and Validation Data

To assess the accuracy of our Landsat juniper classification map for the entire study area, we created a random stratified sampling design for our study area that would allow us to determine the classification accuracy of all juniper densities. We allocated four strata, which included closed canopy woodlands, buffered closed canopy woodlands, planted shelterbelts, and non-woodland areas. We digitized the closed canopy woodlands and planted shelterbelts in ArcGIS 10.5 following the guidelines demonstrated in (Bauman et al., 2016) using very high spatial resolution (VHSR) 60cm National

Agricultural Imagery Program (NAIP), 2014 and 2016 aerial imagery. In addition to obtaining samples of dense woodland cover, we sought to capture less dense samples of open canopied and sporadic trees. We placed a 90-meter buffer around our digitized closed canopy stratum in ArcGIS 10.5; from visual observations, we determined this to be an appropriate distance for additional captures.

Once we defined all the strata within the study area, we generated random points within ArcGIS 10.5. We then referenced each random point to a Landsat pixel by converting each point to a 30x30 meter polygon and snapping them to the Landsat 8 pixel grid. We characterized each polygon using a combination of VHSR imagery, which included NAIP 2016 and other sources of winter imagery accessed through Google Earth from 2013-2017. Our delineation of samples included the recording of the land cover type, juniper presence/absence, and the relative percent of juniper cover. We obtained 1,643 juniper presence and 2,275 juniper absence points for the assessment of pixel-level classification accuracy at different juniper densities.

We created an additional dataset for model training consisting of juniper and non-juniper metrics. We began by supplementing our previous accuracy assessment dataset with an additional 1,000 points. We created new random sampling points in ArcGIS 10.5 that we evenly distributed to our closed canopy woodland and buffered closed canopy woodlands strata. We then delineated the new supplemental points by following the previously mentioned delineation steps. Our new dataset included a combination of our accuracy assessment points and supplemental points. We then removed points from the new dataset that had juniper density greater than 15 percent to represent 865 low-density juniper present and 2,468 juniper absent points (Figure 3-2). Finally, we executed a

sampling process in ArcGIS 10.5, which extracted values from our predictor variables for a final model training dataset.

Juniper Encroachment Model

A random forests classifier is an ensemble-learning algorithm (Breiman, 2001). This approach has been used in developing susceptibility models (Chen et al., 2017; Ismail et al., 2010; Wang et al., 2015; Youssef et al., 2016) has also been applied to numerous predictive applications and across multiple disciplines (Belgiu and Drăguţ, 2016; Biau and Scornet, 2016; Prasad et al., 2006).

The random forests algorithm begins by separating input data into two groups. The first group consists of two thirds of the dataset and is used as internal training samples (in-bag samples), while the remaining one third of the dataset (out-of-the bag sample) is used for cross-validation and estimating the out-of-bag (OOB) error. The in-bag samples individually trains a decision tree without pruning and splitting each node by using a user-defined number of predictor variables (Mtry). This process is repeated multiple times until a user-defined number of decision trees (Ntree) is reached. Each decision tree rule is used to cast a vote on a test feature with the maximum number of voters for the target becoming the final classification. (Breiman, 2001).

We built our random forests model using R statistical software version 3.4.1 (R Core Team, 2017) and the randomForest package (Liaw and Wiener, 2002). We set our Ntree value to 500, as a preliminary analysis showed a good stabilization in the errors before our maximum tree number was attained. Our Mtry value was set as the default, which is the square root of the total number of the predictor variables used in the model.

Model Assessment

We used the Hosmer-Lemeshow goodness-of-fit test to evaluate our model calibration. This test has been commonly used in risk and susceptibility modeling (Bai et al., 2010; Catry et al., 2010; Fang et al., 2013). Hosmer-Lemeshow test categorizes subgroups (referred to as deciles of risk) and performs a Pearson chi-square statistic on the estimated expected and observed frequencies. A close relation of the expected and observed frequencies reflects a model with good fit (Hosmer and Lemeshow, 2000).

We also evaluated model predictions for our low-density juniper model using receiver operating characteristics (ROC). ROC examines multiple classifying cutpoints by plotting the probability of detecting a true positive (sensitivity) against a false positive (1-specificity) (Hosmer and Lemeshow, 2000). A curve is then generated, allowing us to assess the area under the curve (AUC), which is a measure of discrimination or the likelihood the model will predict target and non-target sites. Hosmer and Lemeshow (2000) suggest AUC values represent discrimination as being none (0.5), acceptable (0.7-0.8), excellent (0.8-0.9), or outstanding (0.9-1.0).

We investigated the model performance of a full model and compared it to the performance of models with manually removed variables (Plant, 2012). We implemented this task in an effort to eliminate unnecessary variables while improving our final model computation time. We first began by removing strongly correlated predictor variables followed by a trial and error process in which we independently excluded the remaining variables. We found the final model to have as much predictive power as our full model with a minimal effect on the modeling error.

Results

Juniper Classification

Our final Landsat juniper classification map (Figure 3-3) represented juniper and non-juniper for the entire study area. We identified the true positive detection rate (i.e. the proportion of referenced positives that are correctly classified as positives) of juniper by using our accuracy assessment dataset and grouping the points by juniper density. The true positive and false negative rate in Figure 3-4 indicated a decrease in classification accuracy as juniper density within the pixel decreased. True positive rate for juniper was 90% and greater when pixels contained a juniper density above 50 percent. Once juniper density dropped below 50 percent, the true positive rate decreased to 87% for juniper between 40-50 percent, 77% for juniper between 30-40 percent, 63% for juniper between 20-30 percent, and 43% for juniper between 10-20 percent. As the juniper decreased to 1-10 percent density, the true positive rate was minimal at 11%. The summary classification assessment for our Landsat 8 juniper classification map shown in Table 3-3 indicates overall accuracy (OA) was respectively 94% when evaluated using all juniper densities greater than 15 percent.

Juniper Encroachment Model

Our full model obtained an out-of-bag (OOB) error rate of 15.33%. After removing correlated and redundant variables our final model contained eight predictor variables: distance to juniper, percent juniper, total annual precipitation, percent slope, percent agriculture, soil available water storage, mean annual temperature, and aspect.

The OOB estimate of error rate for our final model was 15.2% and showed as much predictive accuracy as our full model. Our overall random forest error rate shown in Figure 3-5 indicates when the model is applied to a new data source; the model is estimated to have an overall prediction accuracy of 84.4%. In addition, our model obtained an OOB class error rate of 7.2% for non-juniper (juniper absence) and 36.9% for low-density juniper (juniper presence).

The variable importance of the final eight predictor factors are listed in Table 3-3 by descending order of mean decrease in accuracy. Distance to juniper was observed to have the highest conditional importance in our model (51.71) with a strong negative relationship between low-density juniper and the distance to a seed source (Figure 3-7a). We observed low-density junipers with larger distances (> 1000 meters) from a seed source were typically immature planted sources and were not associated with mature trees. Juniper percentage (36.81) had the second to highest importance with a strong positive relationship (Figure 3-7b), which suggested there was an increase in low-density juniper when multiple mature seed sources were in near proximity. Total annual precipitation (28.99) was observed to have a negative relationship (Figure 3-7c) and was followed by percent slope (26.40) with a positive relationship (Figure3-7d) and percent agriculture (25.11) with a negative relationship (Figure 3-7e). Our three variables with lowest importance included soil available water storage (15.67) with a negative relationship (Figure 3-7f), mean annual temperature (13.14) with a positive relationship (Figure 3-7g), and aspect with the lowest importance (6.86) and no evident relationship (Figure 3-7h).

We used the Hosmer-Lemeshow goodness-of-fit test to evaluate the calibration of our final model. The P-value for the Hosmer-Lemeshow test was greater than 0.05 (χ^2 = 5.8565, df = 8, P-value = 0.6633) signifying the final model was well calibrated. We also used the ROC to evaluate model predictions, and accuracy was high with an AUC of 0.884 (Figure 3-8). The Hosmer-Lemeshow test and AUC results indicated that the final low-density juniper model was a good predictor of low-density juniper distributions.

We used the final low-density juniper model to produce our juniper susceptibility map shown in Figure 3-9. We reclassified the map into five groups: very low (0.000-0.075), low (0.075-0.176), moderate (0.176-0.380), high (0.380-0.694), and very high (0.694-1.000) using the Jenks natural breaks system. Our juniper susceptibility map was able to represent areas of encroaching juniper (Figure 3-10b, d) that were not classified as juniper by our Landsat juniper classification map (Figure 3-10a, c). Our juniper susceptibility map characterized the unclassified areas as being of moderate to very high susceptibility. In conjunction with our Landsat juniper map, Table 3-4 shows an additional 62.6% of the study area was characterized as being at very low susceptibility, 20.3% was at low susceptibility, 9.4% at moderate susceptibility, 4.6% at high susceptibility, and 3.1% at very high susceptibility. These results indicate a total of 177,003 ha were at high to very high susceptibility of juniper encroachment in addition to that of what has already been classified.

Discussion

Our final Landsat juniper classification map exhibited a high overall classification accuracy (OA) of 94%, which is comparable with previous juniper mapping studies

(Sankey et al., 2010; Wang et al., 2017; Wylie et al., 2000). However, we found that the probability of detecting juniper decreases as juniper density decreases within a pixel, which Wang et al. (2017) also observed. When juniper density was between 10-20 percent, the detection probability (i.e. true positive rate) was marginal at 43% while juniper densities below ten percent remained relatively undetected with an 11% detection probability. Even though detection probability was low for low-density juniper, our Landsat juniper classification map played a key role in the mapping of low-density juniper susceptibility by generating the top two predictor variables: distance to juniper and juniper density. These variables, in combination with climate, land use, soil characteristics, and topographical factors allowed us to obtain a high prediction accuracy for our low-density juniper model with an area under the curve (AUC) of 0.884. With the accurate prediction of juniper distributions, we have the ability to map present juniper distribution and highlight areas that are at risk of future encroachment.

The likelihood of correctly classifying a pixel as containing juniper decreased as the juniper density within a pixel decreased. This effect was more prevalent once juniper density within pixels decreased below 50 percent. Wang et al. (2017) had similar results as they observed a 90% detection probability for eastern redcedar density above 60 percent and a gradual decrease in detection probability once eastern redcedar density decreased below 60 percent. Failure to identify juniper pixels was suspected to be an influence of juniper height and the omission of woodlands that did not meet their definition of a forest (Wang et al., 2017). However, in this study the inability to consistently capture low-density juniper (< 20 percent) was influenced by the threshold designated during our classification process. Lowering the threshold can result in an

increase in the misclassification of pixels (i.e. false positives), as lower matched filtering values can be associated with pixels that contain multiple spectral signatures. As the number of spectral signatures within the pixel increase, there is a higher potential for the partial spectral unmixing classification to confuse the spectral signatures of the target signature (i.e. juniper) for similar or more dominate signatures within that pixel (i.e. non-juniper). Nonetheless, this level of assessment is still beneficial to juniper management as it allows for the targeting of established juniper sites with the notion that as juniper density increases so does the ecological impact (Chapman et al., 2004; Pierce and Reich, 2010; Frost and Powell, 2011).

Our Landsat juniper classification map allowed us to extract predictor variables that greatly influenced the low-density juniper model. This was not totally unexpected as low-density juniper stands are usually associated with seed dispersal from established juniper sites (Holthuijzen et al., 1987; Yao et al., 1999). Holthuijzen and Sharik (1985) were able to show that within abandoned fields, eastern redcedar density decreased as the distance from a seed source increased. This finding would support our susceptibility map as having very high susceptibility indices for sites close to dense juniper pixels and decreasing indices with increasing distance from established juniper. Additionally, Owensby et al. (1973) saw a significant increase in the establishment of eastern redcedars within fields that were already heavily invaded due to an increase in reproducing individuals. This would suggest areas with a higher percent juniper would contain a higher number of seed producing individuals and in turn would increase the likelihood for new juniper establishment.

Although predictor variables related to juniper cover received the highest conditional importance within our model, climatic and topographical factors had effects as well. The 30 year normal of total annual precipitation had the third highest importance within our model, while mean annual temperature was second to last. We observed a slight negative affect for precipitation of which Owensby et al. (1973) found precipitation to have a statistically significant effect on eastern redcedar encroachment, indicating for every additional inch of precipitation the invasion rate was decreased by 0.2 trees per acre. Mean annual temperature was not a large influencing factor as we only observed a four-degree difference between our 30 year norms (46-50 °F) across the study area. Within our model, we also observed differences in the effects of topographical factors as percent slope was fourth in conditional importance and aspect was found to have the least importance. Eastern redcedar can be associated with moderate to steep slopes (Anderson, 2003), which can contain shallow soils and provide less competition and protection from fire **(**Bryant, 1989; Pierce and Reich, 2010). Some studies have shown aspect to influence juniper establishment (Lawson, 1990; Schmidt and Stubbendieck, 1993), whereas others have shown aspect to have no influence on juniper establishment (Tunnell et al., 2004). In our study, aspect was the least important conditioning factor and no evident relationship. Variable importance ranking for our remaining variables fell considerably below that of our highest ranked variables, yet removal from the model resulted in a slight reduction in model performance.

Our random forest model achieved high overall prediction accuracy, an indication of a well performing model. Our model contained the lowest error for non-juniper, which accounts for the majority of the study area. Model error for low-density juniper was

higher than that of non-juniper sites, but still showed considerable improvement for depicting low-density juniper when compared to using our Landsat juniper classification map alone. A higher model error for low-density juniper reflected our inability to account for specific factors that also influence juniper establishment. Such factors that have been shown to be influential to juniper establishment include livestock grazing practices (Van Auken, 2009; Owensby et al. 1973; Schmidt and Stubbendieck 1993), which can influence the rate of eastern redcedar establishment. With the inclusion of more detailed data on land use practices and additional types of disturbances (e.g., cultivation, haying, and pasture abandonment), it may be possible to increase low-density susceptibility accuracy by accounting for the colonization patterns associated with such disturbances (Yao et al., 1999).

Our Landsat juniper classification maps allowed us to characterize current distributions of established juniper within our study area while also giving us information to support the prediction of low-density juniper. The association between an increase in juniper density and the time and cost of efficiently managing juniper encroachment emphasizes the need to focus on low-density sites (Bidwell et al 2002; Ortmann el al., 1998). By implementing proactive measures, as well as defining appropriate management methods on established juniper, managers can efficiently and effectively address juniper encroachment. Predictive maps such as the ones generated this study can support these efforts by highlighting areas in the landscape that currently have the greatest risk of juniper encroachment to prioritize them for proactive management.

Figures

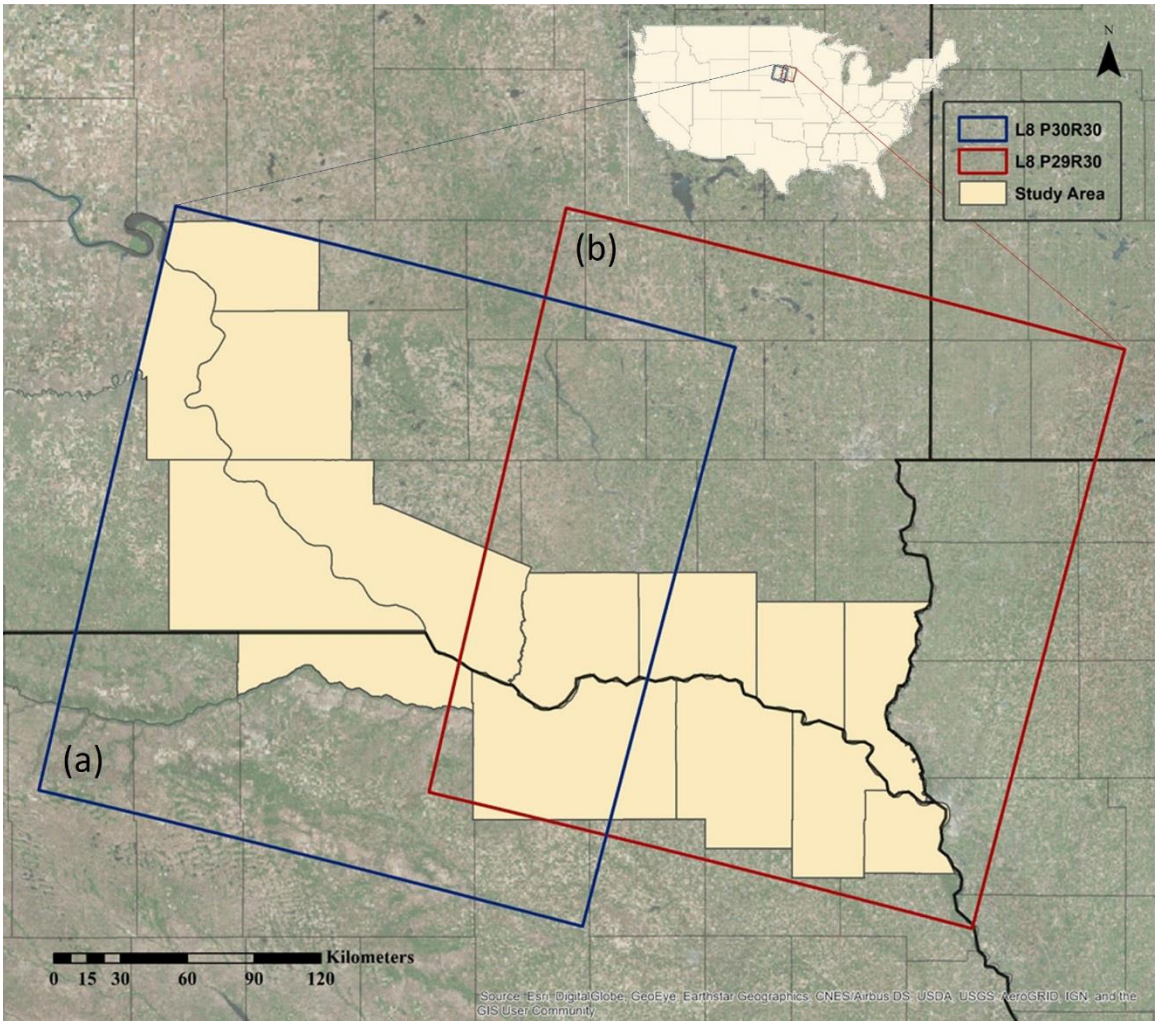

Figure 3-1. Study area composed of nine counties in southeastern South Dakota and five counties in northeastern Nebraska. Landsat 8 OLI path/rows: 30/30 (a) and 29/30 (b) cover the 14 contiguous counties.

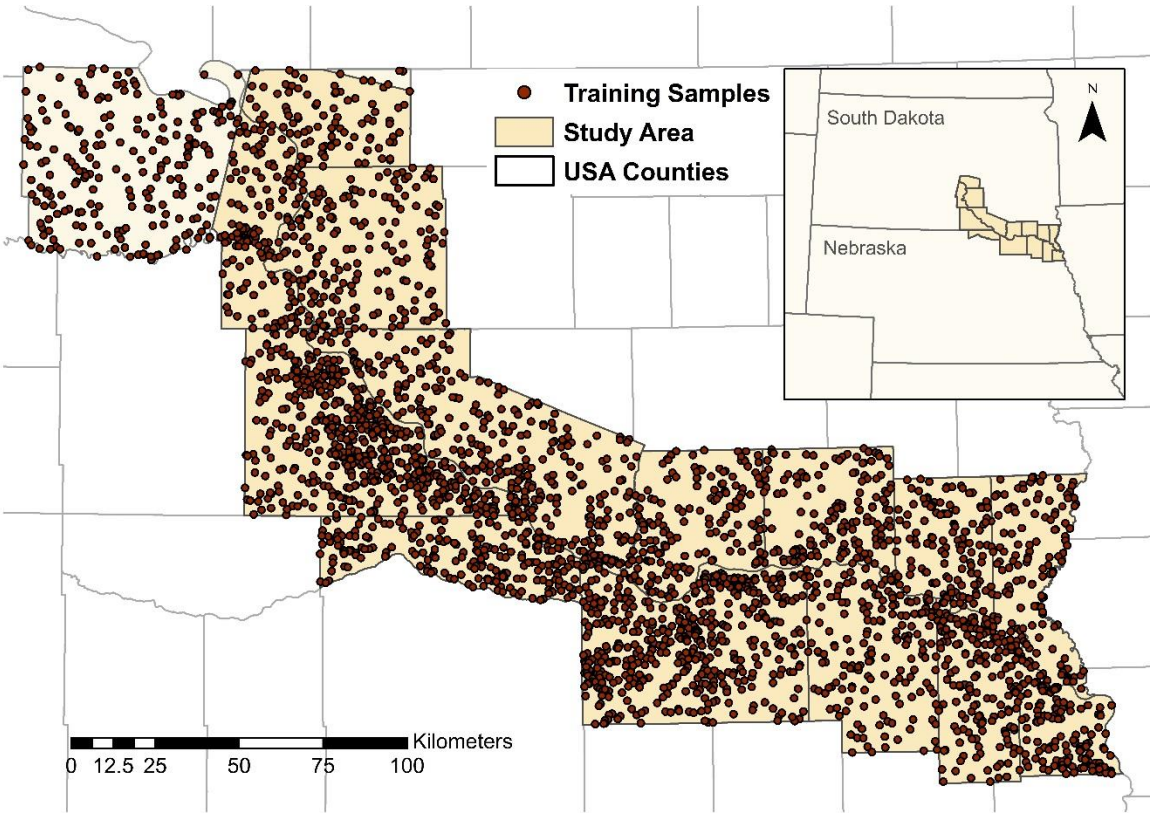

Figure 3-2. Model training samples for random forests low-density juniper model.

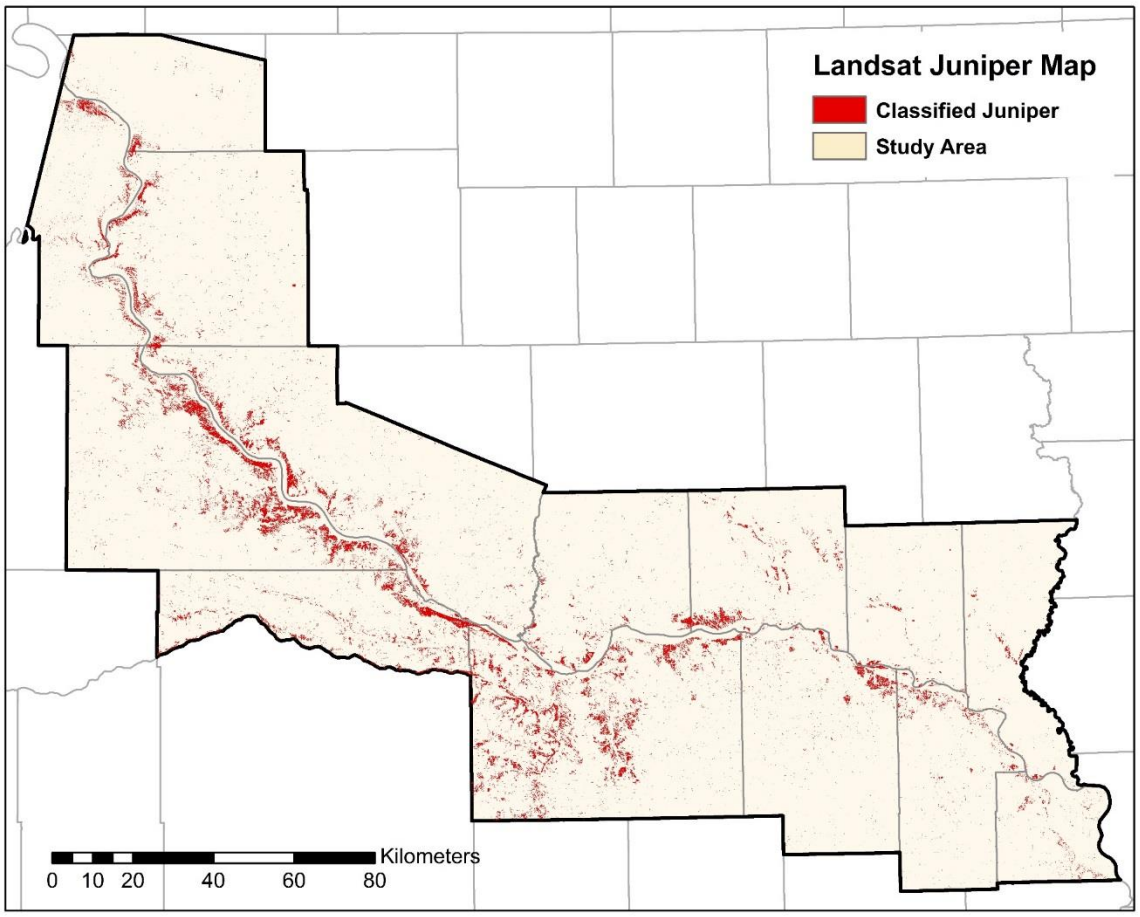

Figure 3-3. Landsat 8 juniper classification map derived from consistent snow covered winter imagery.

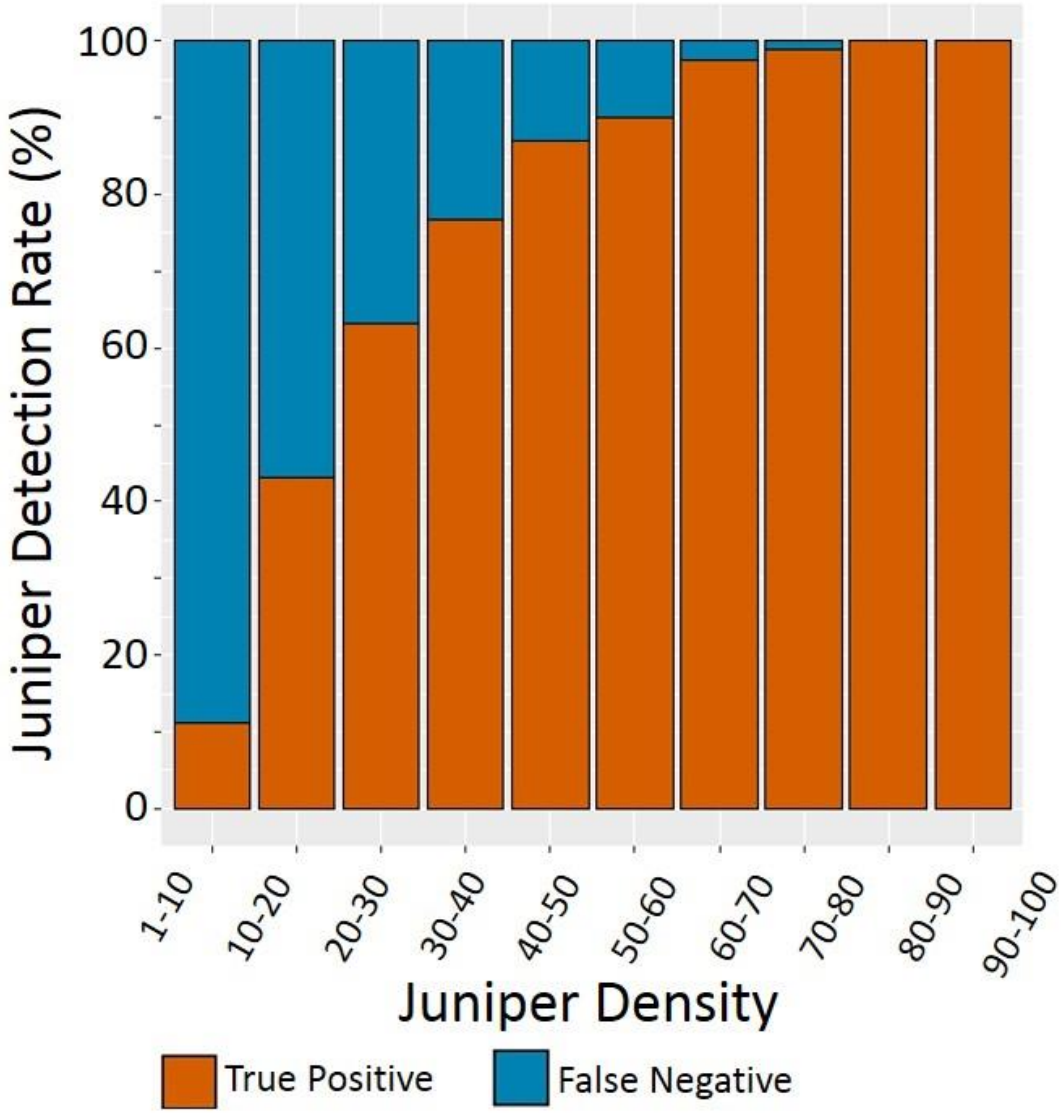

Figure 3-4. Pixel-level quality assessment for juniper classification by density.

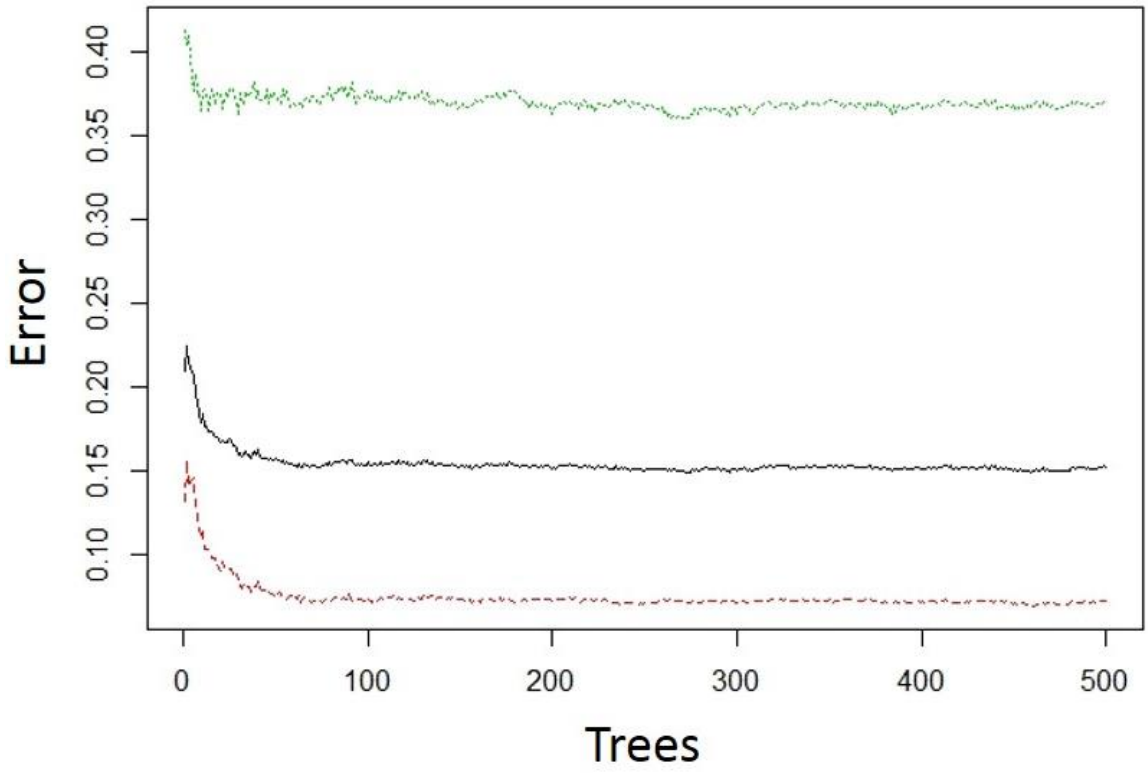

Figure 3-5. The error rate for low-density juniper model (out-of-bag (OOB; black line); juniper absence (red line); and juniper presence (green line)).

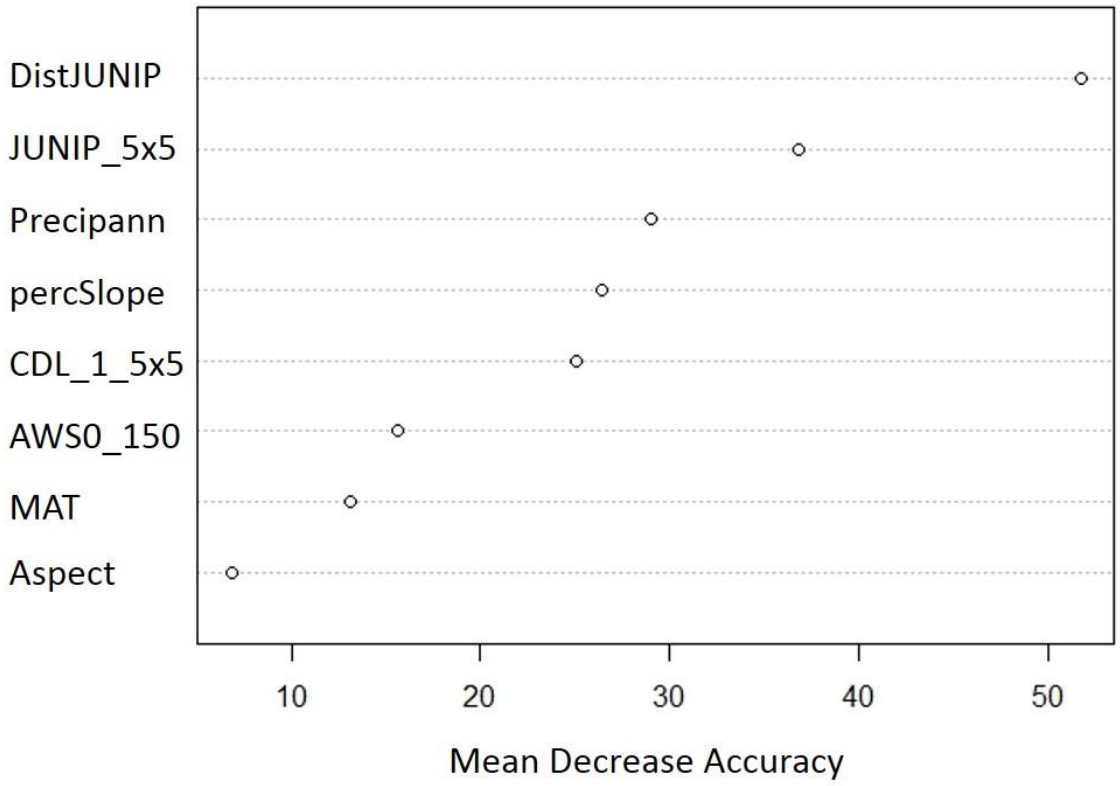

Figure 3-6. Mean decrease accuracy of final eight low-density conditioning factors (listed in descending order) assigned by our random forests model. The eight predictor variables listed are in correspondence of distance to juniper, percent juniper, total annual precipitation, percent slope, percent agriculture, soil available water storage, mean annual temperature, and aspect.

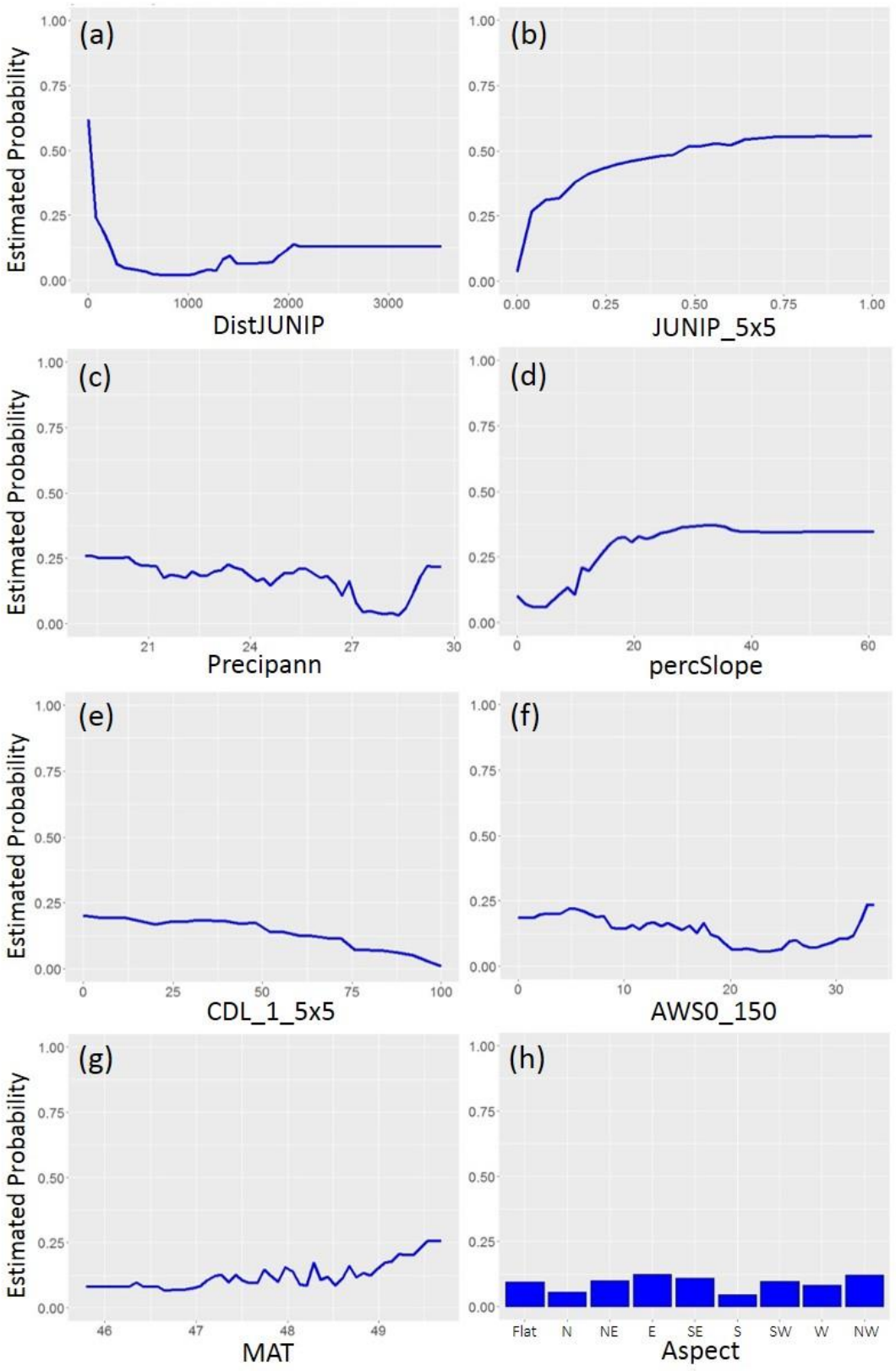

Figure 3-7. Partial dependence plots for eight predictor variables used in the final random forests model for predicting low-density juniper.

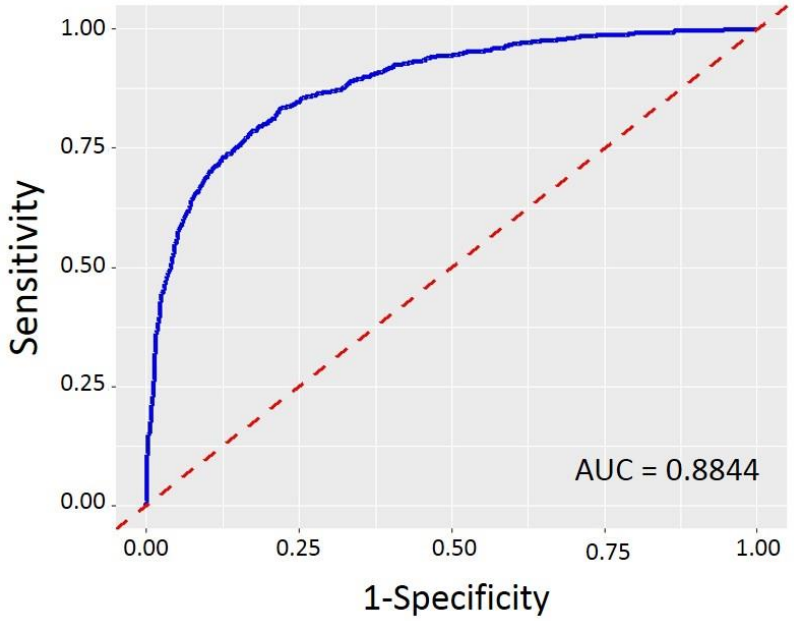

Table 3-8. ROC curve to validate low-density juniper model.

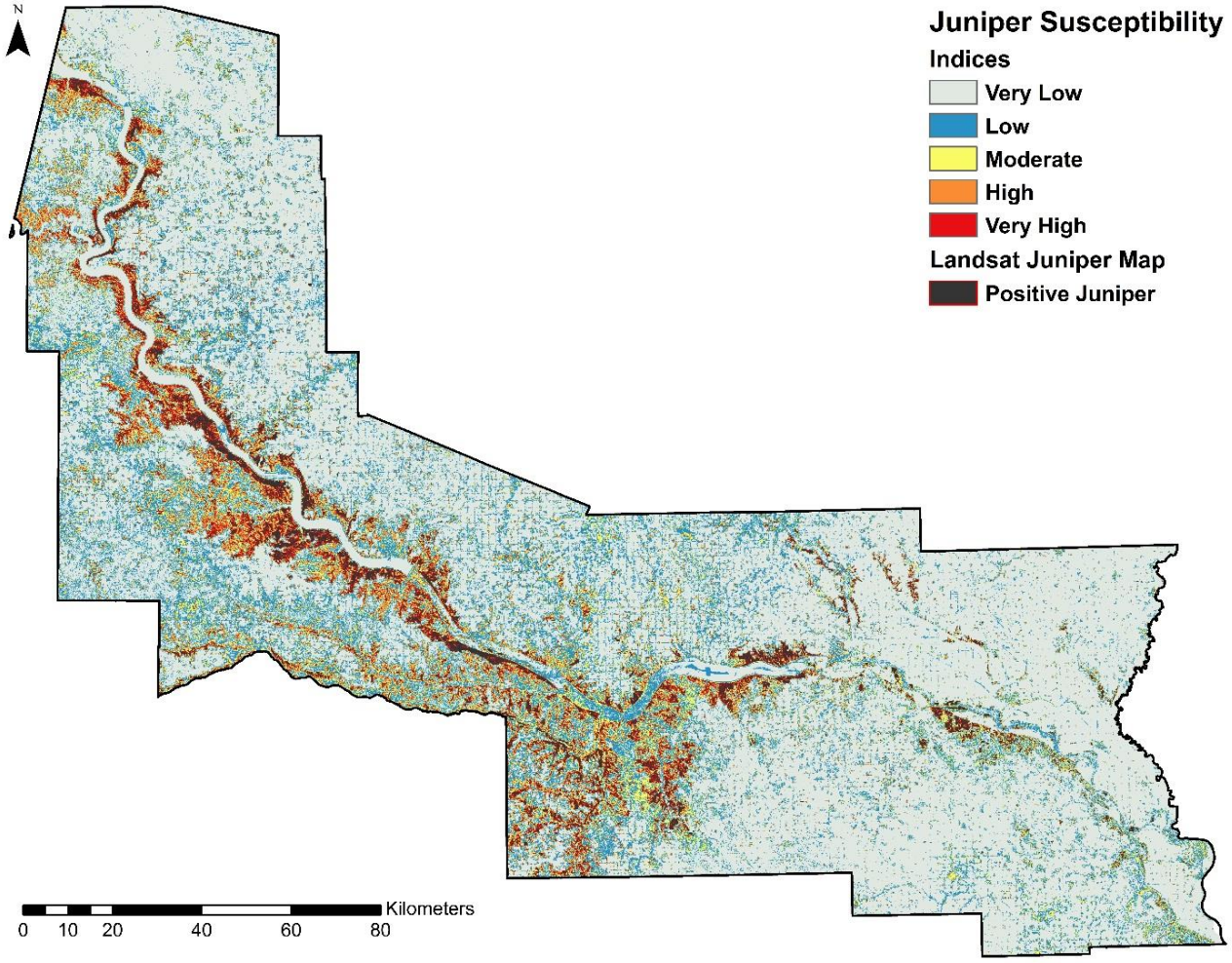

Figure 3-9. Juniper susceptibility map covering the study area. Level of juniper susceptibility is represented by five indices, while including the positive juniper classifications.

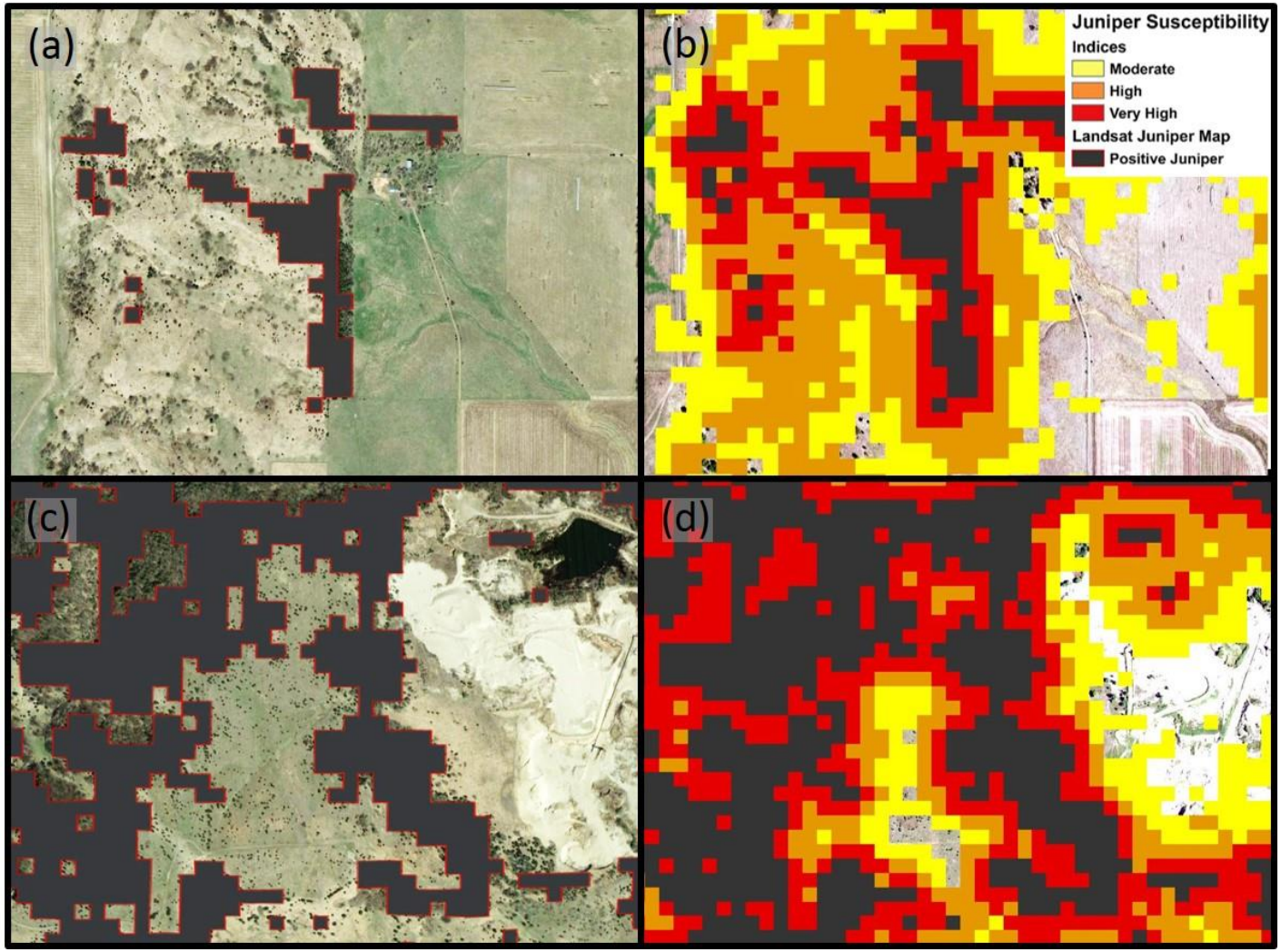

Figure 3-10. A close up view of the juniper susceptibility map. (a, c) show low-density juniper missed by the Landsat images, while (b, d) show the low-density being represented by the juniper susceptibility map.

Tables

Table 3-1. Landsat 8 OLI Surface Reflectance Level-2 imagery used for the classification of juniper. Cloud cover and snow cover represent the percent of the scene covered by either cloud or snow/ice.

Product Identifier	Date	Path/row	Cloud cover	Snow cover
LC08_L1TP_029030_20150107_20170302_01_T2	2015/01/07	29/30	1.55	94.75
LC08_L1TP_030030_20160101_20180131_01_T1	2016/01/01	30/30	0.05	97.91

Table 3-2. Summary of variables included in random forests low-density juniper model. Type of data and measurement scales for variables includes: Nominal (N), Ordinal (O), Interval (I), and Ratio (R).

Variable	Scale	Data Source	Description
Response variable			
JUNIP	N	VHSR Imagery	Presence/absence of juniper
Predictor variables			
Aspect	O	DEM	Compass direction for which a slope faces (from 1: Level/flat; 2: North to 9: Northwest)
percSlope	R	DEM	Percent slope (rise divided by the run, multiplied by 100)
Precipann	R	PRISM	total annual precipitation (cm)
MAT	I	PRISM	Mean annual temperature (°F)
AWS0_150	R	gSSURGO	Available water storage estimate in standard zone 5 (0-150 cm depth; cm)
rootznemc	R	gSSURGO	Depth within the soil profile roots can effectively extract water and nutrients for growth
DRAINCLASS	O	gSSURGO	Natural drainage conditions of the soil by the frequency and duration of wet periods.
SAND	R	gSSURGO	Percent sand
SILT	R	gSSURGO	Percent silt
CLAY	R	gSSURGO	Percent clay
DEP2RESALYR	R	gSSURGO	Depth to restricted layer in soil profile
CDL_1_5x5	R	CDL	Percent agriculture pixels within a 5x5 window; includes: cultivated, hayed, and alfalfa
DistJUNIP	R	Juniper Map	Euclidean distance to juniper pixel (m)
JUNIP_5x5	R	Juniper Map	Percent of juniper pixels within a 5x5 window
DistWATER	R	NHD	Euclidean distance to a water body (m)

Table 3-3. Accuracy assessment of Landsat juniper classification map based on characterized juniper presence and juniper absence pixels. Assessments are evaluated using all juniper densities greater than 15 percent. Shown underlined, overall accuracy (OA) represents the total classification accuracy for both juniper presence and juniper absence pixels.

Classified pixel data	Reference pixel data			User Accuracy (UA)
	Juniper absence	Juniper presence	Row totals	
Juniper absence	2256	183	2439	0.9250
Juniper presence	18	770	788	0.9772
Column totals	2274	953	3227	
Producer accuracy (PA)	0.9921	0.8080		0.9377

Table 3-4. Summary of juniper susceptibility indices covering the study area.

Susceptibility Indices	Pixels	Hectares	Percent cover (%)
Very Low	15920793	1432871.3	62.6
Low	5152010	463680.9	20.3
Moderate	2384631	214916.8	9.4
High	1172905	105561.5	4.6
Very High	793794	71441.46	3.1

CHAPTER 4

THESIS CONCLUSIONS

Overview

The rapid encroachment of woody plants is a threat to the remaining prairies of the Great Plains (Engle et al., 2008). An ecosystem that was once heavily converted to croplands (Samson and Knopf, 1994) is now being converted to woodlands (Briggs et al., 2002b; Norris et al., 2001). The monitoring of woody plant encroachment is essential in order to assess current and future risks while allowing for effective management planning. We evaluated the accuracy of juniper classification maps for southeastern South Dakota and northeastern Nebraska and developed a workflow that allows for continuous and large-scale juniper monitoring. We also modeled the distribution of low-density juniper and determined the prediction accuracy based on juniper metrics and additional ecological factors with which juniper is associated. Finally, we used our low-density juniper model to map the locations at highest risk of future juniper encroachment across the study area. These methods are can be extended to different areas and the information obtained through these maps gives agencies and land managers the ability to more proactively address juniper encroachment in the northern Great Plains.

Objectives 1 & 2

Our first two objectives were to develop a practical workflow for large-scale juniper mapping using Landsat 8 Operational Land Imager (OLI) imagery and partial unmixing techniques and compare the classification accuracies from the resulting map based on different juniper density thresholds and different types of imagery. Our overall

assessments support the use of partial unmixing techniques with snow covered Landsat 8 imagery for mapping juniper. Our use of a single source of multispectral, optical-infrared remote sensing data and partial unmixing methods allowed us to obtain a high overall classification accuracy of 94%, when using winter imagery. Our accuracy was comparable to studies that used multi-source data (Sankey et al., 2010; Wang et al., 2017) and hyperspectral data (Wylie et al., 2000). We successfully captured pixels containing juniper density above 50 percent with a high detection probability and retained an adequate detection rate for pixels containing juniper density above 15 percent. These quantitative pixel level classification results are comparable to Wang et al. (2017) who also saw a loss in the detection probability once pixel level juniper density decreased below 20 percent. We applied our methods to two Landsat scenes (path/rows: 29/30 and 30/30) and obtained comparable results. This study ultimately allowed us to accurately map juniper over a large assessment area with the use of a single source data when other data sources and methods were inapplicable.

Through visual and quantitative assessment, overall classification accuracies were highest for non-growing season Landsat images. This finding was visually apparent as our matched filtering classification of growing season images exhibited a misrepresentation of both juniper and non-juniper sites. We attributed this to a less significant variation in the observed spectral signatures between juniper and other actively growing vegetation within these months (i.e. April-June). Wang et al. (2017) was able to show these spectral differences between junipers and other actively growing vegetation with the use of vegetation indices such as normalized difference vegetation index (NDVI) and enhanced vegetation index (EVI). We also observed that pixels

surrounding juniper that contained snow in the months of January-March had higher reflectance values than those that contained the juniper, allowing us to obtain better separation of juniper and non-juniper. Dozier and Painter (2004) and Vikhamar and Solberg (2003) stated that snow covered pixels contain higher reflectance values in the visible wavelengths and near-infrared wavelengths. If we compare that to the reflectance values of the juniper stands, it is the contrary as we see lower reflectance values in the visible wavelengths and near-infrared wavelengths. Overall, classification results for images containing either snow or no snow during the winter months (January-March) were similar, however when snow cover was constant the pixel level juniper true positive rate increased.

Objective 3

Our third objective was to develop a predictive spatial model for the distribution of low-density juniper based on distance to seed source and environmental covariates and determine the prediction accuracy. We used random forests to construct our low-density juniper model. Our initial full model obtained an out-of-bag (OOB) estimate of error rate of 15.33%. By removing correlated and redundant variables, we were able to improve our final model computation time with no influence on our final model predictive accuracy as we obtained an OOB of 15.2%. Our final model contained eight ecological predictors, which included distance to juniper, percent juniper, total annual precipitation, percent slope, percent agriculture, soil available water storage, mean annual temperature, and aspect. When we compared the prediction of low-density juniper of our model to the Landsat juniper classification map, we found a considerable improvement in accuracy.

Though model predictions of low-density juniper were still below that of our high-density classifications, the model accurately predicated areas that did not have low-density juniper, which accounted for the majority of the study area. Overall model fit was good and prediction accuracy was high as we obtained an area under the curve (AUC) of 0.884, which indicated a strong capability to discriminate between sites with and without low-density juniper. With an accurate map of high-density juniper distributions and the additional ability to account for low-density juniper, we were able to assess present juniper status and future juniper susceptibility to encroachment.

Even though Landsat juniper classification map did not reliably identify areas with low juniper densities, it allowed us to extract our top two predictor variables for low-density juniper: distance to juniper and juniper density. These two factors greatly influenced our low-density juniper model, as low-density juniper is commonly found in close proximity to established juniper stands (Holthuijzen and Sharik, 1985; Holthuijzen et al., 1987; Yao et al., 1999). In addition to these juniper variables, total annual precipitation was found to have the third highest importance within our model. This environmental factor has previously been shown to have a slight influence on the rate of juniper encroachment (Owensby et al., 1973). Other ecological factors such as slope have been influential to juniper establishment, as steeper slopes tend to have shallower soils provide areas of less competition, allowing juniper to establish more easily (Anderson, 2003; Bryant, 1989; Pierce and Reich, 2010). Percent slope was fourth in variable importance and was followed by percent agriculture, soil available water storage, mean annual temperature, and aspect. Even though the remaining variables were not ranked as

high in variable importance, removal of the variable resulted in an increase in the model error and a decrease in the low-density juniper predictive accuracy.

Objective 4

Our fourth objective was to use the resulting maps to evaluate the extent of current juniper establishment and the risk of future encroachment. We were able to incorporate our low-density juniper model and our conditional rasters to develop juniper susceptibility indices that applied to our study area. Our indices represented juniper susceptibility; values closer to zero reflected very low susceptibility and values closer to one reflected very high susceptibility. We reclassified our final susceptibility map into five groups: very low, low, moderate, high, and very high using the Jenks natural break system. The study area was then assessed with a majority of the area at a very low susceptibility.

Through visual assessments of the five susceptibility indices, we obtained a better understanding of what our low-density juniper susceptibility map represented (Appendix A). Sites within our study area that were assessed with a susceptibility of very high were observed to contain established juniper ranging in densities from 1 to 100 percent. These sites represented pixels that contained high density of juniper that were captured with our Landsat juniper classification map in addition to low-density juniper sites (< 20 percent) which were not captured through our juniper classification methods. High susceptibility indices indicated areas that were prone to low-density juniper establishment as they contained low-density juniper or were in close vicinity of established juniper trees. Moderate susceptibility indices contained a low proportion of low-density juniper pixels

primarily between 1 to 10 percent densities. Though a majority of these moderate susceptibility sites did not contain juniper, they were near an encroaching edge and do deserve the attention of managers when preventative juniper encroachment procedures are warranted (i.e. prescribed burns, mowing, and haying). Low susceptibility indices contained a low number of low-density juniper and were more associated with sites of an increased distance from established juniper or near edges of sites that were observed to undergo regular disturbances (i.e. crop cultivation or hayed fields). Very-low susceptibility was indicated for areas located long distances from established juniper or were primarily sites that were observed to undergo regular disturbances.

Our moderate to very-high juniper susceptibility indices reflect both areas that contain juniper and are of at some risk of juniper encroachment within a relatively short time frame. The start of this time frame is designated by the dated imagery of which is used during the juniper classification procedures. Our juniper susceptibility map allows for managers to target and monitor areas of juniper susceptibility while giving them the ability to better designate the appropriate management procedures by investigating the extent and degree of juniper susceptibility within a specific area. In addition, with the ability to capture established juniper and the ability to assign risk to an areas susceptibility to juniper encroachment, managers can make an educated assessment to the total area affected by juniper.

With our Landsat juniper classification map, we found the study area to be occupied by approximately 3.5% juniper. When we investigated our juniper susceptibility map, we perceived areas of high to very high risk of future juniper encroachment (low-density juniper) as being twice the size of that which is already classified as juniper by

our Landsat juniper classification map. The total area at risk of juniper encroachment equates to the potential loss of acres doubling to that of what is already lost to the previously classified juniper. The total loss of acres in our study area to juniper would be nearly half the number of acres already occupied by juniper within eight states for 2012 (Meneguzzo and Liknes, 2015). As juniper density and encroachment increases, the time and cost associated with managing juniper increases (Bidwell et al 2002; Ortmann el al., 1998). As we continue to observe an increase in the areas susceptible to low-density juniper and the rising costs associated with an increasing juniper density, we express the need for the management of these areas susceptible to juniper encroachment.

Management Implications

The results of our research support the use of matched filtering of Landsat 8 Landsat 8 OLI (Operational Land Imager) Level-2 imagery for classifying juniper in the northern Great Plains. We recommend the use of images containing consistent snow coverage during the non-growing months (January-March) as that is when overall classification accuracies were highest. We note there may be challenges with acquiring adequate images during these months that follow those conditions, as consistent snow cover is limited and cloud cover may be high. Therefore, images obtained during the non-growing season containing no snow cover are adequate as long as they maintain a homogenous appearance (no anomalies or growing vegetation). If this approach is taken, we would emphasize the potential for an increase in the misclassification of non-juniper sites unless non-juniper sites (i.e. cultivated fields, waterbodies, etc.) are masked from the image.

Identification of low-density juniper is essential for implementing proactive management practices. By implementing prescribed burns and haying in response to areas at the most risk, managers can prevent additional acres lost to juniper encroachment. However, the probability of detecting low-density juniper with medium resolution imagery (i.e. Landsat) decreases as the juniper density decreases. Once juniper density is below ten percent the probability of detection becomes minimal. Therefore, we recommend the combined use of a Landsat juniper classification combined with prediction of low-density juniper from ecological models. A low-density juniper map allows for the representation of juniper encroachment risk at the landscape scale and allows managers to obtain the information needed to target high-risk areas for carryout the necessary proactive measures. By targeting the appropriate management methods on juniper susceptible and established sites, managers can efficiently and effectively maintain juniper encroachment in the northern Great Plains.

Our practical workflow and juniper classification data will allow for the continuous monitoring of juniper encroachment while establishing a baseline for further studies. Increasing the monitoring zone to additional areas experiencing an expanding juniper include but are not limited to: the Nebraska Sand Hills and into western portions of Nebraska, counties of Pennington, Meade, Haakon, and Ziebach bordering the Cheyenne River of South Dakota. As areas containing higher densities of juniper were mentioned, multiple areas across both states contain small and scattered pockets of juniper, which pose a potential risk of future expansion. With an appropriate monitoring program set in place for regions with high concentrations of juniper and defining

secluded areas, land managers can work with local and state policy makers in establishing an appropriate framework focused around the management of juniper.

The dynamics of juniper encroachment at a state level has only recently been studied in the southern Great Plains (Wang et. al., 2018) and is yet to be evaluated in the northern Great Plains. With the use of recent juniper distributions maps and replicable mapping methods, the assessment of juniper distributions over multiple historical time periods will allow for the indication of juniper encroachment patterns as well as illustrate the direction juniper encroachment is headed. With the knowledge of the dynamics for juniper encroachment in the northern Great Plains, land managers will be able to build upon the predictive model presented in this study, allowing for stronger predictive power in defining areas susceptible to juniper encroachment.

REFERENCES

Anadón, J.D., Sala, O.E., Turner, B.L. and Bennett, E.M., 2014. Effect of woody-plant encroachment on livestock production in North and South America. *Proceedings of the National Academy of Sciences*, *111*(35), pp.12948-12953.

Anderson, J.J. and Cobb, N.S., 2004. Tree cover discrimination in panchromatic aerial imagery of pinyon-juniper woodlands. *Photogrammetric Engineering & Remote Sensing*, *70*(9), pp.1063-1068.

Anderson, M.D., 2003. Juniperus virginiana. *Fire Effects Information System, US Department of Agriculture, Forest Service, Rocky Mountain Research Station, Fire Sciences Laboratory (Producer)*.

Axmann, B.D. and Knapp, A.K., 1993. Water relations of Juniperus virginiana and Andropogon gerardii in an unburned tallgrass prairie watershed. *The Southwestern Naturalist*, pp.325-330.

Bai, S.B., Wang, J., Lü, G.N., Zhou, P.G., Hou, S.S. and Xu, S.N., 2010. GIS-based logistic regression for landslide susceptibility mapping of the Zhongxian segment in the Three Gorges area, China. *Geomorphology*, *115*(1-2), pp.23-31.

Barker, W.T. and Whitman, W.C., 1988. Vegetation of the northern Great Plains. Rangelands, *10*(6), pp.266-272.

Bauman, P., Carlson, B. and Butler, T., 2016. Quantifying Undisturbed (Native) Lands in Eastern South Dakota: 2013. South Dakota State University Extension, Brookings, SD.

Belgiu, M. and Drăguţ, L., 2016. Random forest in remote sensing: A review of applications and future directions. *ISPRS Journal of Photogrammetry and Remote Sensing*, *114*, pp.24-31.

Biau, G. and Scornet, E., 2016. A random forest guided tour. *Test*, *25*(2), pp.197-227.

Bidwell, T.G., Weir, J.R. and Engle, D.M., 2002. Eastern Redcedar Control and Management: Best Management Practices to Restore Oklahoma's Ecosystems. Division of Agricultural Sciences and Natural Resources, Oklahoma State University.

Bragg, T.B. and Hulbert, L.C., 1976. Woody plant invasion of unburned Kansas bluestem prairie. *Journal of Range Management*, *29*(1), pp.19-24.

Breiman, L., 2001. Random forests. *Machine learning*, *45*(1), pp.5-32.

Briggs, J.M., Knapp, A.K. and Brock, B.L., 2002a. Expansion of woody plants in tallgrass prairie: a fifteen-year study of fire and fire-grazing interactions. *The American Midland Naturalist*, *147*(2), pp.287-294.

Briggs, J.M., Hoch, G.A. and Johnson, L.C., 2002b. Assessing the rate, mechanisms, and consequences of the conversion of tallgrass prairie to Juniperus virginiana forest. *Ecosystems*, 5(6), pp.578-586.

Bryant, W.S., 1989. Redcedar (Juniperus virginiana L.) communities in the Kentucky River gorge area of the Bluegrass Region of Kentucky. *USDA Forest Service general technical report NC-North Central Forest Experiment Station (USA)*.

Boardman, J.W., Kruse, F.A. and Green, R.O., 1995. Mapping target signatures via partial unmixing of AVIRIS data.

Buehring, N., Santelmann, P.W. and Elwell, H.M., 1971. Responses of eastern red cedar to control procedures. *Journal of Range Management*, pp.378-382.

Burkman, B., 2009. Forest inventory and analysis sampling and plot design. FIA Fact Sheet Series.

Caterina, G.L., Will, R.E., Turton, D.J., Wilson, D.S. and Zou, C.B., 2014. Water use of Juniperus virginiana trees encroached into mesic prairies in Oklahoma, USA. *Ecohydrology*, *7*(4), pp.1124-1134.

Catry, F.X., Rego, F.C., Bação, F.L. and Moreira, F., 2010. Modeling and mapping wildfire ignition risk in Portugal. *International Journal of Wildland Fire*, *18*(8), pp.921-931.

Chapman, R.N., Engle, D.M., Masters, R.E. and Leslie Jr, D.M., 2004. Tree invasion constrains the influence of herbaceous structure in grassland bird habitats. *Ecoscience*, *11*(1), pp.55-63.

Chen, W., Xie, X., Wang, J., Pradhan, B., Hong, H., Bui, D.T., Duan, Z. and Ma, J., 2017. A comparative study of logistic model tree, random forest, and classification and regression tree models for spatial prediction of landslide susceptibility. *Catena*, *151*, pp.147-160.

Dozier, J. and Painter, T.H., 2004. Multispectral and hyperspectral remote sensing of alpine snow properties. *Annu. Rev. Earth Planet. Sci.*, *32*, pp.465-494.

Engle, D.M., Coppedge, B.R. and Fuhlendorf, S.D., 2008. From the dust bowl to the green glacier: human activity and environmental change in Great Plains grasslands. In *Western North American Juniperus Communities*, Springer, New York, NY, pp. 253-271.

Fang, L.Q., Li, X.L., Liu, K., Li, Y.J., Yao, H.W., Liang, S., Yang, Y., Feng, Z.J., Gray, G.C. and Cao, W.C., 2013. Mapping spread and risk of avian influenza A (H7N9) in China. *Scientific reports*, *3*, p.2722.

Franklin, S.E., 2001. *Remote sensing for sustainable forest management*. Boca Raton, FL: CRC Press.

Frost, J.S. and Powell, L.A., 2011. Cedar infestation impacts avian communities along the Niobrara River Valley, Nebraska. *Restoration Ecology*, *19*(4), pp.529-536.

Fuhlendorf, S.D., Archer, S.A., Smeins, F., Engle, D.M. and Taylor, C.A., 2008. The combined influence of grazing, fire, and herbaceous productivity on tree–grass interactions. In *Western North American Juniperus Communities*, Springer, New York, NY, pp. 219-238.

Gehring, J.L. and Bragg, T.B., 1992. Changes in prairie vegetation under eastern red cedar (Juniperus virginiana L.) in an eastern Nebraska bluestem prairie. *American Midland Naturalist*, pp.209-217.

Ganguli, A.C., Engle, D.M., Mayer, P.M. and Fuhlendorf, S.D., 2008. When are native species inappropriate for conservation plantings?. *Rangelands*, *30*(6), pp.27-32.

Giri, C.P., 2012. *Remote sensing of land use and land cover: principles and applications*. Boca Raton, FL: CRC Press.

Greene, S.L. and Knox, J.C., 2014. Coupling legacy geomorphic surface facies to riparian vegetation: Assessing red cedar invasion along the Missouri River downstream of Gavins Point dam, South Dakota. *Geomorphology*, *204*, pp.277-286.

Heilman, G.E., Strittholt, J.R., Slosser, N.C. and Dellasala, D.A., 2002. Forest Fragmentation of the Conterminous United States: Assessing Forest Intactness

through Road Density and Spatial Characteristics: Forest fragmentation can be measured and monitored in a powerful new way by combining remote sensing, geographic information systems, and analytical software. *AIBS Bulletin*, *52*(5), pp.411-422.

Holthuijzen, A.M. and Sharik, T.L., 1985. The avian seed dispersal system of eastern red cedar (Juniperus virginiana). *Canadian Journal of Botany*, *63*(9), pp.1508-1515.

Holthuijzen, A.M., Sharik, T.L. and Fraser, J.D., 1987. Dispersal of eastern red cedar (Juniperus virginiana) into pastures: an overview. *Canadian Journal of Botany*, *65*(6), pp.1092-1095.

Hosmer, D.W. & Lemeshow, S., 2000. Applied logistic regression 2nd ed., New York: Wiley.

Hutcheson, H.L. and Rothe, S.C., 1977. Eastern redcedar (Juniperus virginiana) reproduction and spread in Brookings County, South Dakota. In Proceedings of the South Dakota Academy of Science.

Ismail, R., Mutanga, O. and Kumar, L., 2010. Modeling the potential distribution of pine forests susceptible to sirex noctilio infestations in Mpumalanga, South Africa. *Transactions in GIS*, *14*(5), pp.709-726.

Knapp, A.K., Briggs, J.M., Collins, S.L., Archer, S.R., Bret-Harte, M.S., Ewers, B.E., Peters, D.P., Young, D.R., Shaver, G.R., Pendall, E. and Cleary, M.B., 2008. Shrub encroachment in North American grasslands: shifts in growth form dominance rapidly alters control of ecosystem carbon inputs. *Global Change Biology*, *14*(3), pp.615-623.

Knezevic, S., Melvin, S., Gompert, T. and Gramlich, S., 2005. Integrated management of eastern redcedar. *Lincoln, NE, USA: University of Nebraska Lincoln Extension EC186. Google Scholar*.

Kottek, M., Grieser, J., Beck, C., Rudolf, B. and Rubel, F., 2006. World map of the Köppen-Geiger climate classification updated. *Meteorologische Zeitschrift*, *15*(3), pp.259-263.

Lawson, E.R. 1990. *Juniperus virginiana* L. eastern redcedar. In *Silvics of North America*, vol. I: Conifers, tech. coord. R.M. Burns and B.H. Honkala, USDA Forest Service, Washington, DC, *Agricultural Handbook, 654*, pp.131-40.

Liaw, A. and Wiener, M., 2002. Classification and regression by randomForest. *R news*, *2*(3), pp.18-22.

McKinley, D.C. and Blair, J.M., 2008. Woody plant encroachment by Juniperus virginiana in a mesic native grassland promotes rapid carbon and nitrogen accrual. *Ecosystems*, *11*(3), pp.454-468.

Meneguzzo, D.M., Butler, B.J., Crocker, S.J., Haugen, D.E., Moser, W.K., Perry, C.H., Wilson, B.T. and Woodall, C.W., 2008. Nebraska's forests, 2005. *Resour. Bull. NRS-27. Newtown Square, PA: US Department of Agriculture, Forest Service, Northern Research Station.*, *27*, pp.94.

Meneguzzo, D.M. and Liknes, G.C., 2015. Status and trends of eastern redcedar (Juniperus virginiana) in the central United States: Analyses and observations based on Forest Inventory and Analysis data. *Journal of Forestry*, *113*(3), pp.325-334.

Meneguzzo, D.M. 2017. Forests of Nebraska, 2016. *Resource Update FS-114. Newtown Square, PA: U.S. Department of Agriculture, Forest Service, Northern Research Station*, *114*, pp.1-5.

NOAA: National Centers for Environmental Information. Data Tools: U.S. Normals Data (1981-2010). < https://gis.ncdc.noaa.gov/maps/ncei/normals> Accessed 9 Jan 2018.

Noble, D.L., 1990. Juniperus scopulorum Sarg. Rocky Mountain juniper. In *Silvics of North America*, vol. I: Conifers, tech. coord. R.M. Burns and B.H. Honkala, USDA Forest Service, Washington, DC, *Agricultural Handbook, 654*, pp.116-126.

Norris, M. D., Blair, J. M., and Johnson, L. C., 2001. Land cover change in eastern Kansas: litter dynamics of closed-canopy eastern redcedar forests in tallgrass prairie. *Canadian Journal of Botany*, *79*(2), pp.214-222.

NRCS, 2017. US Department of Agriculture, National Resources Conservation Service, Geospatial Data Gateway. Available from: <http://datagateway.nrcs.usda.gov>, Accessed 17 Dec. 2017.

O'Connell, B.M., Conkling, B.L., Wilson, A.M., Burrill, E.A., Turner, J.A., Pugh, S.A., Christensen, G., Ridley, T. and Menlove, J., 2017. The forest inventory and analysis database: database description and users guide for phase 2, version 7.0. *USDA Forest Service, North Central Research Station*.

Oklahoma Conservation Commission, 2008. *Eastern redcedar invading the landscape. Fact sheet*. Oklahoma City, OK, USA: Oklahoma Conservation Commission, pp.4.

Ormsbee, P., Bazzaz, F.A. and Boggess, W.R., 1976. Physiological ecology of Juniperus virginiana in oldfields. *Oecologia*, *23*(1), pp.75-82.

Ortmann, J., Stubbendieck, J., Masters, R.A., Pfeiffer, G.H. and Bragg, T.B., 1998. Efficacy and costs of controlling eastern redcedar. *Journal of Range Management*, pp.158-163.

Ortmann, J., Stubbendieck, J. and Mitchell, R., 2007. Integrated Management of Eastern Redcedar on Grasslands. *University of Nebraska-Lincoln Cooperative Extension Publication*.

Owensby, C.E., Blan, K.R., Eaton, B.J. and Russ, O.G., 1973. Evaluation of eastern redcedar Infestations in the northern Kansas Flint Hills. *Journal of Range Management*, pp.256-260.

Pierce, A.M. and Reich, P.B., 2010. The effects of eastern red cedar (Juniperus virginiana) invasion and removal on a dry bluff prairie ecosystem. *Biological Invasions*, *12*(1), pp.241-252.

Pimentel, D., Zuniga, R. and Morrison, D., 2005. Update on the environmental and economic costs associated with alien-invasive species in the United States. *Ecological economics*, *52*(3), pp.273-288.

Plant, R.E., 2012. *Spatial data analysis in ecology and agriculture using R*. cRc Press.

Poznanovic, A.J., Falkowski, M.J., Maclean, A.L., Smith, A. and Evans, J.S., 2014. An accuracy assessment of tree detection algorithms in juniper woodlands. *Photogrammetric Engineering & Remote Sensing*, *80*(7), pp.627-637.

Prasad, A.M., Iverson, L.R. and Liaw, A., 2006. Newer classification and regression tree techniques: bagging and random forests for ecological prediction. *Ecosystems*, *9*(2), pp.181-199.

PRISM Climate Group, 2017, PRISM Gridded Climate Data, Oregon State University, Available from: < http://prism.oregonstate.edu>, Accessed 9 Jan 2018.

R Core Team (2017). R: A language and environment for statistical computing. R Foundation for Statistical Computing, Vienna, Austria. Available from: <https://www.R-project.org/>.

Ratajczak, Z., Nippert, J.B. and Collins, S.L., 2012. Woody encroachment decreases diversity across North American grasslands and savannas. *Ecology*, *93*(4), pp.697-703.

Roberts, C.P., Uden, D.R., Allen, C.R. and Twidwell, D., 2018. Doublethink and scale mismatch polarize policies for an invasive tree. *PloS one*, *13*(3), p.e0189733.

Ruefenacht, B., Finco, M.V., Nelson, M.D., Czaplewski, R., Helmer, E.H., Blackard, J.A., Holden, G.R., Lister, A.J., Salajanu, D., Weyermann, D. and Winterberger, K., 2008. Conterminous US and Alaska forest type mapping using forest inventory and analysis data. *Photogrammetric Engineering & Remote Sensing*, *74*(11), pp.1379-1388.

Samson, F. and Knopf, F., 1994. Prairie conservation in North America. *BioScience*, *44*(6), pp.418-421.

Samson, F.B. and Knopf, F.L. eds., 1996. *Prairie conservation: preserving North America's most endangered ecosystem*. Island Press.

Samson, F., Knopf, F. & Ostlie, W., 2004. Great Plains ecosystems: past, present, and future. *Wildlife Society Bulletin*, *32*(1), pp.6–15.

Sankey, T.T. and Germino, M.J., 2008. Assessment of juniper encroachment with the use of satellite imagery and geospatial data. *Rangeland Ecology & Management*, *61*(4), pp.412-418.

Sankey, T.T., Glenn, N., Ehinger, S., Boehm, A. and Hardegree, S., 2010. Characterizing western juniper expansion via a fusion of Landsat 5 Thematic Mapper and lidar data. *Rangeland ecology & management*, *63*(5), pp.514-523.

Sankey, T. and Glenn, N., 2011. Landsat-5 TM and lidar fusion for sub-pixel juniper tree cover estimates in a western rangeland. *Photogrammetric Engineering & Remote Sensing*, *77*(12), pp.1241-1248.

Schmidt, T.L. and Stubbendieck, J., 1993. Factors influencing eastern redcedar seedling survival on rangeland. *Journal of Range Management*, pp.448-451.

Simberloff, D., 2003. How much information on population biology is needed to manage introduced species?. *Conservation Biology*, *17*(1), pp.83-92.

Simonsen, V.L., J.E. Fleishmann, D. Whisenhunt, J.D. Volesky, and D. Twidwell. 2015. Act now or pay later: Evaluating the cost of reactive versus proactive Eastern Redcedar management. University of Nebraska-Lincoln Extension.

Smith, S., 2011. *Eastern red-cedar: positives, negatives and management*. Samuel Roberts Noble Foundation, pp.1-8.

Soil Science Division Staff, 2017. Soil survey manual. C. Ditzler, K. Scheffe, and H.C. Monger (eds.). USDA Handbook 18. Government Printing Office, Washington, D.C.

Starks, P. J., Venuto, B. C., Dugas, W. A., and Kiniry, J., 2014. Measurements of canopy interception and transpiration of eastern redcedar grown in open environments. *Environment and Natural Resources Research*, *4*(3), pp.103.

Twidwell, D., Rogers, W.E., Fuhlendorf, S.D., Wonkka, C.L., Engle, D.M., Weir, J.R., Kreuter, U.P. and Taylor, C.A., 2013. The rising Great Plains fire campaign: citizens' response to woody plant encroachment. *Frontiers in Ecology and the Environment*, *11*(s1).

Tunnell, S.J., Stubbendieck, J., Huddle, J. and Brollier, J., 2004. Seed dynamics of eastern redcedar in the mixed-grass prairie. *Great Plains Research*, pp.129-142.

USDA Farm Service Agency, 2018, National Agriculture Imagery Program (NAIP), Available from <https://www.fsa.usda.gov/programs-and-services/aerial-photography/imagery-programs/naip-imagery/index>, Accessed 01 Apr. 2018

USDA Forest Service, 2018. Forest Inventory and Analysis National Program. Available from: <https://www.fia.fs.fed.us/tools-data/>, Accessed 31 Jan. 2018.

USDA-NASS Cropland Data Layer, 2016. Published crop-specific data layer. Available from: <https://nassgeodata.gmu.edu/CropScape/>, Accessed 11 Dec. 2017.

USDA-NRCS, 2017. *Cost-share programs for conservation tree planting in Nebraska. Fact sheet*. Available from: <http://www.ne.nrcs.usda.gov/programs>, Accessed 01 May. 2018.

USGS Earth Explorer, 2017. US Geological Survey Earth Explorer, Available from: <http://earthexplorer.usgs.gov>, Accessed 3 May 2017.

USGS NHD, 2017, National Hydrography Dataset. Available from: <https://nhd.usgs.gov/data.html>, Accessed 11 Nov. 2017.

Van Auken, O.W., 2009. Causes and consequences of woody plant encroachment into western North American grasslands. *Journal of environmental management*, *90*(10), pp.2931-2942.

Van Haverbeke, D.F. and Read, R.A., 1976. Genetics of eastern redcedar. *USDA Forest Serv. Res. Pap.*, (WO-32).

Vikhamar, D. and Solberg, R., 2003. Subpixel mapping of snow cover in forests by optical remote sensing. Remote Sensing of Environment, *84*(1), pp.69-82.

Walker, T.L. and Hoback, W.W., 2007. Effects of invasive eastern redcedar on capture rates of Nicrophorus americanus and other Silphidae. *Environmental entomology*, *36*(2), pp.297-307.

Walters, Brian F. 2017. Forests of South Dakota, 2016. Resource *Update FS-110. Newtown Square, PA: U.S. Department of Agriculture, Forest Service, Northern Research Station*, 4 p., *110*, pp.1-4.

Wang, J., Xiao, X., Qin, Y., Dong, J., Geissler, G., Zhang, G., Cejda, N., Alikhani, B. and Doughty, R.B., 2017. Mapping the dynamics of eastern redcedar encroachment into grasslands during 1984–2010 through PALSAR and time series Landsat images. *Remote sensing of environment*, *190*, pp.233-246.

Wang, J., Xiao, X., Qin, Y., Doughty, R.B., Dong, J. and Zou, Z., 2018. Characterizing the encroachment of juniper forests into sub-humid and semi-arid prairies from

1984 to 2010 using PALSAR and Landsat data. *Remote Sensing of Environment*, *205*, pp.166-179.

Wang, Z., Lai, C., Chen, X., Yang, B., Zhao, S. and Bai, X., 2015. Flood hazard risk assessment model based on random forest. *Journal of Hydrology*, *527*, pp.1130-1141.

Wilson, J. and Schmidt, T., 1990. Controlling eastern redcedar on rangelands and pastures. *Rangelands*, *12*(3), pp.156-158.

Wimberly, M.C., Narem, D.M., Bauman, P.J., Carlson, B.T. and Ahlering, M.A., 2018. Grassland connectivity in fragmented agricultural landscapes of the north-central United States. *Biological Conservation*, *217*, pp.121-130.

Wulder, M.A., Dymond, C.C., White, J.C., Leckie, D.G. and Carroll, A.L., 2006. Surveying mountain pine beetle damage of forests: A review of remote sensing opportunities. *Forest Ecology and management*, *221*(1-3), pp.27-41.

Wulder, M.A., Masek, J.G., Cohen, W.B., Loveland, T.R. and Woodcock, C.E., 2012. Opening the archive: How free data has enabled the science and monitoring promise of Landsat. *Remote Sensing of Environment*, *122*, pp.2-10.

Wulder, M.A., White, J.C., Loveland, T.R., Woodcock, C.E., Belward, A.S., Cohen, W.B., Fosnight, E.A., Shaw, J., Masek, J.G. and Roy, D.P., 2016. The global Landsat archive: Status, consolidation, and direction. *Remote Sensing of Environment*, *185*, pp.271-283.

Wylie, B.K., Meyer, D.J., Choate, M.J., Vierling, L., Kozak, P.K. and Green, R.O., 2000. Mapping woody vegetation and eastern red cedar in the Nebraska Sand Hills

using AVIRIS. In *AVIRIS Airborne Geoscience Workshop. JPL Publication 00-18. Pasadena, CA: Jet Propulsion Laboratory, California Institute of Technology*.

Yao, J., Holt, R.D., Rich, P.M. and Marshall, W.S., 1999. Woody plant colonization in an experimentally fragmented landscape. *Ecography*, *22*(6), pp.715-728.

Yokomizo, H., Possingham, H.P., Thomas, M.B. and Buckley, Y.M., 2009. Managing the impact of invasive species: the value of knowing the density–impact curve. *Ecological Applications*, *19*(2), pp.376-386.

Youssef, A.M., Pourghasemi, H.R., Pourtaghi, Z.S. and Al-Katheeri, M.M., 2016. Landslide susceptibility mapping using random forest, boosted regression tree, classification and regression tree, and general linear models and comparison of their performance at Wadi Tayyah Basin, Asir Region, Saudi Arabia. *Landslides*, *13*(5), pp.839-856.

Zavaleta, E., 2000. The economic value of controlling an invasive shrub. *AMBIO: a Journal of the Human Environment*, *29*(8), pp.462-467.

Zou, C.B., Turton, D.J., Will, R.E., Engle, D.M. and Fuhlendorf, S.D., 2014. Alteration of hydrological processes and streamflow with juniper (Juniperus virginiana) encroachment in a mesic grassland catchment. *Hydrological Processes*, *28*(26), pp.6173-6182.

Zou, C.B., Qiao, L. & Wilcox, B.P., 2016. Woodland expansion in central Oklahoma will significantly reduce streamflows – a modelling analysis. *Ecohydrology*, *9*(5), pp.807–816.

APPENDICIES

Appendix A. Juniper susceptibility indices and definition of indices represented in juniper susceptibility map.

Indices	Range	Definition
Very Low	0.000-0.075	Areas of increased distances from established juniper and/or are sites that were observed to undergo regular disturbances.
Low	0.075-0.176	Areas of increased distances from established juniper or are near edges of sites that were observed to undergo regular disturbances.
Moderate	0.176-0.380	Areas contain a low number of low-density juniper (1-10%) with a majority of sites not containing juniper but are near an encroaching juniper edge
High	0.380-0.694	Areas that are prone to low-density juniper establishment as they contain low-density juniper (< 20%) or are in close vicinity of established juniper.
Very High	0.694-1.000	Areas contain established juniper ranging in densities from 1 to 100 percent.